

AKR1 Encodes a Candidate Effector of the G $\beta\gamma$ Complex in the *Saccharomyces cerevisiae* Pheromone Response Pathway and Contributes to Control of both Cell Shape and Signal Transduction

PETER M. PRYCIAK* AND LELAND H. HARTWELL

Department of Genetics, University of Washington, Seattle, Washington 98195-7360

Received 9 November 1995/Returned for modification 28 December 1995/Accepted 4 March 1996

Mating pheromones of *Saccharomyces cerevisiae* control both signal transduction events and changes in cell shape. The G $\beta\gamma$ complex of the pheromone receptor-coupled G protein activates the signal transduction pathway, leading to transcriptional induction and cell cycle arrest, but how pheromone-dependent signalling leads to cell shape changes is unclear. We used a two-hybrid system to search for proteins that interact with the G $\beta\gamma$ complex and that might be involved in cell shape changes. We identified the ankyrin repeat-containing protein Akr1p and show here that it interacts with the free G $\beta\gamma$ complex. This interaction may be regulated by pheromone, since Akr1p is excluded from the G $\alpha\beta\gamma$ heterotrimer. Both haploid and diploid cells lacking Akr1p grow slowly and develop deformed buds or projections, suggesting that this protein participates in the control of cell shape. In addition, Akr1p has a negative influence on the pheromone response pathway. Epistasis analysis demonstrates that this negative effect does not act on the G $\beta\gamma$ complex but instead affects the kinase cascade downstream of G $\beta\gamma$, so that the kinase Ste20p and components downstream of Ste20p (e.g., Ste11p and Ste7p) are partially activated in cells lacking Akr1p. Although the elevated signalling is eliminated by deletion of Ste20p (or components downstream of Ste20p), the growth and morphological abnormalities of cells lacking Akr1p are not rescued by deletion of any of the known pheromone response pathway components. We therefore propose that Akr1p negatively affects the activity of a protein that both controls cell shape and contributes to the pheromone response pathway upstream of Ste20p but downstream of G $\beta\gamma$. Specifically, because recent evidence suggests that Bem1p, Cdc24p, and Cdc42p can act in the pheromone response pathway, we suggest that Akr1p affects the functions of these proteins, by preventing them from activating mating-specific targets including the pheromone-responsive kinase cascade, until G $\beta\gamma$ is activated by pheromone.

The mating reaction of *Saccharomyces cerevisiae* provides a model system for studying both signal transduction events and the control of cellular morphology and polarity in response to external cues (for reviews, see references 3, 14, 21, 46, and 76). During the mating process, extracellular signals instruct each partner cell to arrest its division at a particular stage in the cell cycle, to alter its repertoire of gene expression by inducing new transcription, and to alter its morphology in an asymmetric fashion so that it can fuse with its chosen partner to form a diploid zygote. We are particularly interested in this last response, because it implies communication between the pheromone-responsive signal transduction pathway and determinants of cell shape and polarity.

Yeast cells are stimulated to mate when secreted pheromones (α factor and α factor) activate a signal transduction pathway by binding to a seven-transmembrane type of receptor (encoded by the genes *STE2* [α cells] and *STE3* [α cells]) that is coupled to a heterotrimeric G protein (G $\alpha\beta\gamma$, with subunits encoded by the genes *GPA1*, *STE4*, and *STE18*, respectively [reviewed in references 3 and 76]). Genetic data (reviewed in references 3, 33, and 76) suggest that this binding triggers release of the G $\beta\gamma$ complex from the inhibitory G α subunit, allowing G $\beta\gamma$ to transmit signal downstream to a cascade of

protein kinases (Ste20p, Ste11p, Ste7p, and Fus3p or Kss1p), which in turn communicates with determinants of cell cycle arrest (Far1p) and transcriptional induction (Ste12p). In addition, another component required for signal transmission (Ste5p) has recently been suggested to serve as a scaffold for at least the three final members of the kinase cascade (18, 43, 51, 58). Recent biochemical data verify the genetically deduced order of action for this signal transduction pathway and also suggest that most of the members of this pathway have indeed been identified, since each of the kinases will phosphorylate the next kinase in the pathway, and the final kinase(s) will phosphorylate the factors (Ste12p and Far1p) that mediate the different responses to pheromone (24, 26, 56, 57, 89, 91). There is still, however, uncertainty about how the kinase cascade becomes activated by the free G $\beta\gamma$ complex; it is unresolved whether G $\beta\gamma$ activates the kinase cascade directly or through additional, unidentified intermediates.

In addition to activating the signal transduction pathway leading to cell cycle arrest and transcriptional induction, mating cells undergo morphological changes (reviewed in references 14, 21, and 76). Cells in the process of forming a zygote asymmetrically rearrange their cytoskeletons and their distribution of secretory vesicles, and partner cells eventually fuse their cell walls, plasma membranes, and nuclei. Importantly, these responses are not spatially uniform but instead are directed toward the partner cell. That mating yeast cells can respond directionally toward the source of pheromone is demonstrated by their ability to locate and mate preferentially with

* Corresponding author. Department of Genetics, Box 357360, University of Washington, Seattle, WA 98195-7360. Phone: (206) 543-2833. Fax: (206) 543-0754. Electronic mail address: pryciak@u.washington.edu.

a pheromone-producing cell in a mixed environment of pheromone-producing and pheromoneless cells (37–39, 45, 52). In addition, yeast cells will produce projections that grow along gradients of pheromone provided by micropipettes (68). In these ways, the mating response of yeast resembles chemotaxis. This behavior implies that at least some components of the signal transduction pathway inside the cell preserve the spatial information inherent in the distribution of pheromone outside the cell and that one or more of these components communicates with the determinants of cell shape and polarity, so that the direction of polarization is coupled with the direction from which signal is being received.

Cell shape and polarity in *S. cerevisiae* are governed in part by the proteins Bem1p, Cdc24p, and Cdc42p, which are often referred to as polarity establishment proteins because they are necessary for the generation of cell polarity during vegetative growth (5, 12, 13, 73). Cells with mutations in these genes are unable to restrict cell surface growth to the daughter bud and instead expand uniformly. Mutations in these genes also result in poor mating and the inability to undergo normal morphogenesis in response to pheromone (15, 16, 27, 64). Thus, it is likely that in some manner the activities of the polarity establishment gene products are modulated by the pheromone response pathway, but it is unclear which component(s) of the pheromone response pathway performs this function. From studies of the ability of cells to locate and polarize toward the source of pheromone, we had reason to suspect that this process might be controlled by the upstream members of the pheromone response pathway, in a manner independent of signal transmission through the kinase cascade. Specifically, cells lacking members of the kinase cascade (Ste20p, Ste11p, Ste7p, Fus3p, and Kss1p) or the scaffolding protein (Ste5p) retain the ability to distinguish between pheromone-producing and pheromoneless cells, whereas cells lacking the receptor (Ste2p or Ste3p) or G-protein subunits (Gpa1p, Ste4p, and Ste18p) are more defective for this ability (67). Therefore, we suspected that either the receptor, the G α subunit, or the G $\beta\gamma$ complex communicates with determinants of cell polarity, in addition to playing its known role in signal transduction.

In this study, we report our efforts to find gene products that interact with the G $\beta\gamma$ complex and that might participate in the communication between the pheromone response pathway and the determinants of cell shape and polarity. Our observations suggest that G $\beta\gamma$ communicates with a protein, the ankyrin repeat-containing protein Akr1p, that is involved in the control of both signal transmission and cell shape changes. This suggestion is further supported by recent evidence showing that determinants of cell shape, namely, the polarity establishment proteins Bem1p, Cdc24p, and Cdc42p, can participate in signal transduction (42, 71, 77, 90).

MATERIALS AND METHODS

Yeast strains, media, and methods. Standard methods for yeast propagation and manipulation (30) were followed. Standard rich medium (YPD), synthetic complete (SC) medium, and SC medium lacking amino acids or other nutrients were used (69). Yeast strains used are described in Table 1. Strain L40 has been described elsewhere (36); strains 8998-4-3b and 8941-1-4b were generated by K. Schrick; all other strains were generated for this study. Most yeast strains were in the 381G background (*cry1 ade2-1^{oc} ade3 his4-580^{mm} leu2-3,112 lys2^{oc} trp1^{am} tyr1^{oc} ura3-52 SUP4-3^{ts}*); the exceptions are noted in Table 1. Integration of Fus1-LacZ reporter constructs was achieved by transformation of SphI-digested pFC23 and pFL-LYS, which target integration to the *FUS1* locus while leaving the *FUS1* coding region intact. Chromosomal replacement of the *AKR1* gene was achieved by transformation with pUCakr1::URA3 that had been digested with *Bam*HI and *Pst*I and was confirmed in URA3⁺ transformants by PCR (not shown). Strains carrying deletions of pheromone response pathway genes were made either by transformation with pEL36 (*ste4::URA3*) digested with *Eco*RI or with pDJ154 (*ste4::LEU2*) digested with *Pst*I and *Xba*I or by crossing to 381G strains carrying the desired deletions (31, 67) or to W303 strains carrying a

deletion of *STE20* (47). Crosses with strains carrying deletions of pheromone response pathway genes were performed after complementation of their sterility by transformation with p4-9 (*STE4*) or pNC252 (*GAL-STE12*) and then allowing for loss of the plasmid before sporulation. Transformations of yeast strains were done by the lithium acetate method (28).

Plasmids. Plasmids YE24 (8), pG1301 (55), pPGK-SCG1 (41), pDJ154 (31), pCTC52 (called plex-lamin in reference 36), and pEL36 (48) have been previously described. Plasmid pNC252 (a gift from B. Errede) is a 2 μ m *URA3* construct expressing *STE12* under control of a galactose-inducible promoter. Plasmid p4-9 contains the *STE4* gene as isolated from a yeast genomic library constructed in the centromeric *TRP1* vector pM111 (86). Plasmids pFC23 and pFL-LYS, which are integrating vectors expressing a Fus1p-LacZ protein fusion under control of the *FUS1* promoter and are marked with *LEU2* and *LYS2*, respectively, were constructed by replacement of the *URA3*-containing *Hind*III-to-*Stu*I fragment in pSB286 (11) with a *LEU2*-containing *Hind*III-to-*Sma*I fragment (by F. Chang) or a *LYS2*-containing *Hind*III-to-*Eco*RI fragment. Plasmid pRS314-Sph (a gift from H. McDonald) is a derivative of pRS314 (70) in which the *Sac*I site was replaced with an *Sph*I site. Plasmid pHM27 (a gift from H. McDonald) expresses a *lexA* DNA-binding domain (DBD)-*CDC31* fusion in the low-copy-number vector pRS314-Sph. For two-hybrid interaction studies, the parental vectors used were pBTM116 (4), a 2 μ m *TRP1* plasmid for making *lexA* DBD fusions expressed from an *ADH* promoter, and pGAD424 (4), a 2 μ m *LEU2* plasmid for making *GAL4* activation domain (AD) fusions expressed from an *ADH* promoter. All of the cloning steps described below that involved PCR amplification used the proofreading enzyme Vent DNA polymerase (New England Biolabs) except for those involving mutagenic PCR, which used *Taq* DNA polymerase (Promega).

Plasmid pB1a is a centromere (CEN) plasmid expressing a *lexA* DBD-*STE4* fusion that was constructed as follows. The entire *STE4* gene was amplified from plasmid pC5-A19 (59) (isolated from a galactose-inducible genomic DNA library [63] and containing sequences downstream of base 481 of *STE4*), using oligonucleotides YES-Gins (5' CCTCTAGCCGAATTCCTCGAGGCTACGTC 3') and ST4-D3 (5' GGATGTATATTTCTAGAATAGGATCC 3') (*Eco*RI and *Bam*HI sites are underlined); the product was cleaved with *Eco*RI and *Bam*HI and cloned into the corresponding sites in pBTM116 to generate the 2 μ m *lexA* DBD-*STE4* fusion construct pBTM-STE4. Subsequently, the *Sph*I fragment containing the *lexA* DBD-*STE4* fusion under control of the *ADH* promoter was transferred from the 2 μ m plasmid pBTM-STE4 to the *Sph*I site of the centromere plasmid pRS314-Sph to finally generate plasmid pB1a.

Plasmid pGAD-STE4, expressing a *GAL4* AD-*STE4* fusion, was constructed by transferring the *STE4*-containing *Eco*RI-to-*Bam*HI fragment from pBTM-STE4 into the corresponding sites in pGAD424. Plasmids encoding fusions of the *GAL4* AD to mutant derivatives of Ste4p were isolated as follows. Plasmids pGm3-F30 and pGm3-E41, expressing mutant derivatives of Ste4p that are defective for interaction with G γ (*ste4^{gid}*) and G α (*ste4^{aid}*), respectively, were generated by mutagenic PCR amplification (9) of *STE4* sequences by using oligonucleotides YES-Gins and ST4-D55 (5' CGCGAGGATCCGCATGCTCA CAGTAT 3') (*Bam*HI site is underlined), cleavage of the product with *Eco*RI and *Bam*HI, and cloning into the corresponding sites in pGAD424. The resulting library of *GAL4* AD-mutant *ste4* fusions was screened for clones that specifically lost the two-hybrid interaction with either pBTM-STE18 or pBTM-GPA1 but retained interaction with the other (59). Plasmid pGADm3-D10, expressing a *GAL4* AD-*ste4^{gid}* fusion, was constructed by amplification of mutant *ste4* sequences from plasmid pm3-D10 by using oligonucleotides YES-Gins and ST4-D55, cleavage with *Eco*RI and *Bam*HI, and cloning into the corresponding sites in pGAD424; plasmid pm3-D10 contains a galactose-inducible *ste4^{gid}* allele, in the vector pYES-R (25), which was isolated from a screen for *ste4* mutants showing defects in mating (59).

Plasmid pM70-ADE2 is an *ADE2* 2 μ m plasmid expressing the *STE18* gene under control of the *ADH* promoter, constructed by replacing the *URA3*-containing *Bgl*II fragment from pM70p2 (19) with an *ADE2*-containing *Bgl*II fragment from pASZ11 (80). Plasmid pBTM-STE18, expressing a *lexA* DBD-*STE18* fusion, was constructed by amplification of the entire *STE18* coding region from pM70-ADE2, using oligonucleotides ST18-U11 (5' GCCGCGAATTCAGAAT GACATCAGTTC 3') and ST18-D22 (5' CGCTCGGATCCCTCATTACATA AGCGTAC 3') (*Eco*RI and *Bam*HI sites are underlined), cleavage of the product with *Eco*RI and *Bam*HI, and cloning into the corresponding sites in pBTM116.

Plasmid pBTM-GPA1, expressing a *lexA* DBD-GPA1 fusion, was constructed by amplification of the entire *GPA1* coding region from YcpgPA1-lac111 (79), using oligonucleotides GP-URI (5' TATTAAGGTAGGAATTCATCGGGGTG TACAG 3') and GP-DPS (5' AACACTACTTAAATTCCTGCAAGTTCCTTC 3') (*Eco*RI and *Pst*I sites are underlined), cleavage of the product with *Eco*RI and *Pst*I, and cloning into the corresponding sites in pBTM116.

Plasmids p80.Aw3-1, p100.Dw1-3, pST4B.1-1, and pST4B.3-1, expressing *GAL4* AD-*AKR1* fusions in which the fusion junction corresponds to *Sau*3AI sites at positions 210, 295, 295, and 357 of *AKR1*, respectively, were isolated in the two-hybrid screen (see below). Plasmid pBTM-AKR1, expressing a *lexA* DBD-*AKR1* fusion, was constructed by amplification of the region containing codons 22 to 764 of *AKR1* from p80.Aw3-1, using oligonucleotides AKR1-up (5' CGACGCGGGATCCCTAGCAATAACGAC 3') (*Bam*HI site is underlined) and AKR1-dn (5' ATTCAGCGGATCCCTTATAAGAAGCAC 3'), cleavage

TABLE 1. Yeast strains used in this study

Strain	Genotype
PPY433 ^a	a <i>cry1 ade2 his4 leu2 lys2 trp1 ura3 cyh2 SUP4 FUS1::FUS1-lacZ(LYS2)</i>
PPY506 ^a	a <i>cry1 ade2 his4 leu2 lys2 trp1 ura3 cyh2 SUP4 FUS1::FUS1-lacZ(LYS2) akr1::URA3</i>
PPY510 ^a	a <i>cry1 ade2 his4 leu2 lys2 trp1 ura3 cyh2 SUP4 FUS1::FUS1-lacZ(LYS2) akr1::URA3 ste4::LEU2</i>
PPY512 ^a	a <i>cry1 ade2 his4 leu2 lys2 trp1 ura3 cyh2 SUP4 FUS1::FUS1-lacZ(LEU2) akr1::URA3 ste5Δ1::LYS2</i>
PPY497 ^a	a <i>cry1 ade2 ade3 his4 leu2 lys2 trp1 ura3 cyh2 SUP4 FUS1::FUS1-lacZ(LYS2) ste11Δ::hisG</i>
PPY547 ^a	a <i>cry1 ade2 ade3 his4 leu2 lys2 trp1 ura3 cyh2 SUP4 FUS1::FUS1-lacZ(LYS2) akr1::URA3 ste11Δ::hisG</i>
PPY516 ^a	a <i>cry1 ade2 ade3 his4 leu2 lys2 trp1 ura3 cyh2 SUP4 FUS1::FUS1-lacZ(LYS2) akr1::URA3 ste7::LEU2</i>
PPY543 ^a	a <i>cry1 ade2 ade3 his4 leu2 lys2 trp1 ura3 cyh2 SUP4 FUS1::FUS1-lacZ(LYS2) akr1::URA3 fus3Δ::LEU2 kss1Δ::ura3^{FOA}</i>
PPY670 ^a	a <i>cry1 ade2 ade3 his4 leu2 lys2 trp1 ura3 cyh2 SUP4 FUS1::FUS1-lacZ(LYS2) akr1::URA3 ste12Δ::LEU2</i>
PPY617 ^a	a <i>cry1 his4 lys2 trp1 tyr1 ura3 SUP4 FUS1::FUS1-lacZ(LYS2)</i>
PPY618 ^a	a <i>cry1 his4 lys2 trp1 tyr1 ura3 SUP4 FUS1::FUS1-lacZ(LYS2) akr1::URA3</i>
PPY519 ^a	a <i>cry1 his4 lys2 trp1 tyr1 ura3 SUP4 FUS1::FUS1-lacZ(LYS2) far1Δ::URA3</i>
PPY620 ^a	a <i>cry1 his4 lys2 trp1 tyr1 ura3 SUP4 FUS1::FUS1-lacZ(LYS2) akr1::URA3 far1Δ::URA3</i>
PPY600 ^a	a <i>cry1 his4 lys2 trp1 tyr1 ura3 SUP4 FUS1::FUS1-lacZ(LYS2)</i>
PPY603 ^a	a <i>cry1 his4 lys2 trp1 tyr1 ura3 SUP4 FUS1::FUS1-lacZ(LYS2) akr1::URA3</i>
PPY541 ^a	a <i>cry1 his4 lys2 trp1 tyr1 ura3 cyh2 SUP4 FUS1::FUS1-lacZ(LYS2) akr1::URA3 ste20Δ::TRP1</i>
PPY499 ^a	a <i>cry1 his4 lys2 trp1 tyr1 ura3 cyh2 SUP4 FUS1::FUS1-lacZ(LYS2) ste20Δ::TRP1</i>
PPY583 ^a	a/α <i>cry1/cry1 his4/HIS4 leu2/leu2 lys2/lys2 trp1/trp1 ura3/ura3 SUP4/SUP4 FUS1::FUS1-lacZ(LYS2)/FUS1 akr1::URA3/AKR1</i>
PPY584 ^a	a/α <i>cry1/cry1 his4/HIS4 leu2/leu2 lys2/lys2 trp1/trp1 ura3/ura3 SUP4/SUP4 FUS1::FUS1-lacZ(LYS2)/FUS1 akr1::URA3/akr1::URA3</i>
8998-4-3b ^a	α <i>cry1 ade6 his3 leu2 lys2 tyr1 ura3 SUP4</i>
8941-1-4b ^a	α <i>cry1 ade6 his4 leu2 trp1 tyr1 ura3 SUP4 mfx1::URA3 mfx2::LEU2</i>
PPY646 ^b	α <i>ade2-1 his3-11,15 leu2-3,112 trp1-1 ura3-1 can1 FUS1::FUS1-lacZ(LEU2)</i>
PPY647 ^b	α <i>ade2-1 his3-11,15 leu2-3,112 trp1-1 ura3-1 can1 FUS1::FUS1-lacZ(LEU2) akr1::URA3</i>
PPY648 ^b	α <i>ade2-1 his3-11,15 leu2-3,112 trp1-1 ura3-1 can1 FUS1::FUS1-lacZ(LEU2) akr1::URA3 ste20::TRP1</i>
PPY495 ^b	a <i>ade2-1 his3-11,15 leu2-3,112 trp1-1 ura3-1 can1 FUS1::FUS1-lacZ(LEU2)</i>
PPY553 ^b	a <i>ade2-1 his3-11,15 leu2-3,112 trp1-1 ura3-1 can1 FUS1::FUS1-lacZ(LEU2) akr1::URA3</i>
PPY496 ^b	a <i>ade2-1 his3-11,15 leu2-3,112 trp1-1 ura3-1 can1 FUS1::FUS1-lacZ(LEU2) ste20::TRP1</i>
PPY557 ^b	a <i>ade2-1 his3-11,15 leu2-3,112 trp1-1 ura3-1 can1 FUS1::FUS1-lacZ(LEU2) akr1::URA3 ste20::TRP1</i>
PPY653 ^b	a/α <i>ade2-1/ade2-1 his3-11,15/his3-11,15 leu2-3,112/leu2-3,112 trp1-1/trp1-1 ura3-1/ura3-1 can1/can1 FUS1::FUS1-lacZ(LEU2)/FUS1 akr1::URA3/AKR1</i>
PPY651 ^b	a/α <i>ade2-1/ade2-1 his3-11,15/his3-11,15 leu2-3,112/leu2-3,112 trp1-1/trp1-1 ura3-1/ura3-1 can1/can1 FUS1::FUS1-lacZ(LEU2)/FUS1 akr1::URA3/akr1::URA3</i>
PPY189 ^c	a <i>his3-Δ1 trp1-289 ura3-52</i>
PPY529 ^c	a <i>his3-Δ1 trp1-289 ura3-52 akr1::URA3</i>
PPY201 ^d	a <i>his3-Δ200 leu2-3,112 lys2-801 ura3-52</i>
PPY536 ^d	a <i>his3-Δ200 leu2-3,112 lys2-801 ura3-52 akr1::URA3</i>
L40 ^d	a <i>ade2 his3-Δ200 leu2-3,112 trp1-901 LYS2::(<i>lexAop</i>)₄-HIS3 URA3::(<i>lexAop</i>)₈-lacZ</i>
PPY429 ^d	a/α <i>ade2/ade2 his3-Δ200/his3-Δ200 leu2-3,112/leu2-3,112 trp1-901/trp1-901 LYS2::(<i>lexAop</i>)₄-HIS3/lys2 URA3::(<i>lexAop</i>)₈-lacZ/URA3::(<i>lexAop</i>)₈-lacZ met/MET</i>
PPY665 ^d	a <i>ade2 his3-Δ200 leu2-3,112 trp1-901 LYS2::(<i>lexAop</i>)₄-HIS3 URA3::(<i>lexAop</i>)₈-lacZ ste4::URA3</i>
PPY667 ^d	a <i>ade2 his3-Δ200 leu2-3,112 trp1-901 LYS2::(<i>lexAop</i>)₄-HIS3 ura3-52</i>

^a 381G strain background; see Materials and Methods for alleles of markers.

^b W303 strain background.

^c A364A strain background.

^d S288C strain background.

with *Bam*HI and *Pst*I (which cleaves at base 2527 of *AKR1*), and cloning into the corresponding sites in pBTM116. Plasmid pUCakr1::URA3 contains *AKR1* sequences from bases 210 to 2531 (cloned as a *Bam*HI-to-*Pst*I fragment from p80.Aw3-1 into pUC19) in which the *AKR1* sequences from the *Hpa*I site (base 365) to the *Bgl*II site (base 1826) were replaced with a *URA3*-containing *Sma*I-to-*Bgl*II fragment from pM70p2 (19).

Two-hybrid methods. Measurements of two-hybrid interaction were performed with yeast strains L40 (36), PPY429, PPY665, and PPY667 (Table 1). Because the high-copy-number (2μm) DBD-*STE4* fusion construct pBTM-*STE4* gave strong background signal (*His*⁺, β-galactosidase positive) even in the absence of any AD fusion, we created the low-copy-number (CEN) DBD-*STE4* fusion construct pB1a and found that the background signal was now eliminated in haploid tester strains but not in diploid tester strains. This difference between haploid and diploid tester strains is assumed to be due to accumulation of extra copies of the construct in diploid cells, with selective pressure against such accumulation in haploid strains because of the growth disadvantage due to high expression levels of *Ste4p*, which can cause cell cycle arrest by activation of the pheromone response pathway (20, 87). Although we have not proven this assumption to be true, the observation suggested that a potential source of noise in the two-hybrid search would be plasmids that caused the cells either to behave as diploid cells or to become resistant to cell cycle arrest. This expectation was verified, as described below.

For the two-hybrid search, cells of strain L40 that had been previously transformed with the DBD-*STE4* fusion plasmid pB1a (CEN, *TRP1*) were transformed with DNA from six separate AD fusion libraries, all in *LEU2* vectors.

These libraries consisted of yeast genomic DNA that had been partially digested with either *Sau*3AI (17) or a mixture of *Acl*I, *Hin*PI, *Mae*II, *Msp*I, and *Taq*I (a gift from P. James and E. Craig) and then ligated to generate fusions with the *GAL4* AD in each of three different reading frames. A total of 6.7×10^6 cotransformants (1.0×10^6 for the *Sau*3AI libraries and 5.7×10^6 for the mixed enzyme libraries) were screened. Cotransformants were selected by plating on SC medium lacking tryptophan and leucine and then after growth at 30°C for 3 to 4 days were replicated to SC medium lacking histidine, to select for activation of the *lexAop*-*HIS3* reporter.

Roughly half of 1,189 initial *His*⁺ colonies were also β-galactosidase positive and required both the *TRP1* and the *LEU2* plasmid for the positive signal. Of these, poor mating and resistance to α-pheromone-mediated growth arrest suggested that most carried plasmids that caused the cells to behave as diploids or to be otherwise resistant to cell cycle arrest. A sample of 107 clones was checked by Southern hybridization with a probe corresponding to the α2 coding region of the *MATα* locus (not shown), and 98 of these gave positive hybridization, suggesting that the vast majority of the clones isolated gave signal by virtue of causing the cells to behave as α/α diploids. Of the α-pheromone-resistant clones that did not hybridize with the α2 probe, three were sequenced, and these were found to carry truncations of genes which could plausibly give rise to pheromone resistance or diploid character (i.e., carboxy-terminal truncations of *STE18* and amino-terminal truncations of *SIR3* [not shown]). Therefore, we analyzed further only those clones that did not show pheromone resistance or poor mating. Only four total satisfied this criterion, and each of these retested positively after recovery of the plasmid (35) and retransformation into L40, but only when

cotransformed with the DBD-*STE4* fusion plasmid pB1a and not with a control fusion to either lamin C or Cdc31p (pCTC52 or pHM27, respectively). These four were sequenced by using a primer to *GAL4* AD sequences, and sequences were compared with entries in databases by using the BLAST algorithm (2). Each was found to carry an in-frame fusion to the product of the *AKR1* gene, beginning at codons 22, 51, 51, and 71 of Akr1p (corresponding to nucleotide positions 210, 295, 295, and 357 of *AKR1*). These clones were named p80.Aw3-1, p100.Dw1-3, pST4B.1-1, and pST4B.3-1, respectively.

Although we had anticipated recovering the genes *STE18* and *GPA1*, encoding the $\text{G}\gamma$ and $\text{G}\alpha$ subunits of the G protein, the identification of any gene from these libraries necessitates that it contain the restriction site(s) used in the construction of the library; therefore interactions with proteins that are small or that require their extreme amino termini might be particularly difficult to recover. In addition, our requirement that the clones not cause pheromone resistance may have hampered recovery of *GPA1*.

β -Galactosidase assays. Quantitative β -galactosidase assays were carried out as previously described (54, 82). In brief, densities of cell cultures were measured by optical density at 660 nm (OD_{660}), and cells were then harvested either by pelleting 1 ml (two-hybrid assays and Fus1-LacZ dose-response assays) or by filtration of 9 ml (basal Fus1-LacZ assays), resuspended in 0.5 ml of Z buffer (82 mM sodium phosphate [pH 7.0], 10 mM KCl, 1 mM MgSO_4 , 40 mM β -mercaptoethanol), and permeabilized by vortexing in the presence of 0.01 ml of 0.4% sodium dodecyl sulfate and 0.05 ml of chloroform. Reactions were started by addition of 0.3 ml of *o*-nitrophenyl- β -D-galactopyranoside (2.4 mg/ml in Z buffer), incubated at 30°C for 10 to 300 min, stopped by addition of 0.5 ml of 1 M Na_2CO_3 , and then assayed by measurement of OD_{420} . β -Galactosidase activity was calculated in Miller units (54) as $1,000 \times (\text{OD}_{420}/\text{OD}_{660}) \times \text{culture volume (milliliters)} \times \text{reaction time (minutes)}$. Cell cultures used for two-hybrid measurements were grown in SC liquid medium lacking leucine and tryptophan to late log phase (2×10^7 to 8×10^7 /ml). Cell cultures used for Fus1-LacZ assays were grown at 30°C in SC liquid medium to 3×10^6 to 8×10^6 per ml, diluted to 3×10^6 per ml, and allowed to continue growth at 30°C in the absence or presence of added pheromone for 90 to 180 min, depending on the experiment.

Quantitative mating assays. Measurements of mating efficiency and mating partner discrimination were performed as described previously (37, 39). Matings were performed at 30°C for 3 h, using strain 8998-4-3b as the wild-type partner and 8941-1-4b as the pheromoneless partner.

Photomicroscopy. Cell cultures were grown at 30°C in SC liquid medium to 1×10^6 to 6×10^6 /ml, sonicated, and fixed by addition of formaldehyde directly to the culture to a final concentration of 5%. Samples mounted on slides under coverslips were photographed on a Nikon Microphot-FX under differential interference contrast, using a 40 \times oil immersion objective and a 1.6 \times intermediate magnifier.

RESULTS

Identification of *AKR1* as interacting with *STE4*. We hypothesized that in addition to playing its role in activating the pheromone response pathway, the free $\text{G}\beta\gamma$ complex of the G protein might communicate with determinants of cell shape and polarity. Therefore, we used a two-hybrid system to search for proteins that interact with the $\text{G}\beta\gamma$ complex. For this purpose, we initially constructed a 2- μm plasmid carrying a fusion of the *lexA* DBD to full-length *STE4*, encoding the $\text{G}\beta$ subunit. Because this construct gave strong background signal, we transferred the fusion to a CEN plasmid, which eliminated the background (see Materials and Methods). Using this modified version, we searched through 6.7×10^6 total transformants from two different libraries of yeast genomic DNA fragments fused to an AD.

The gene *AKR1* was identified four independent times; no other genes were identified as interacting with Ste4p in this search, although a large number of initial positive clones were eliminated because they activated the latent transcriptional activation ability of the DBD-*STE4* fusion (see Materials and Methods). The four clones identified were all in-frame fusions of the AD to the *AKR1* gene product (GenBank accession number L31407), at codons 22, 51, 51, and 71 of the 764 codon *AKR1* coding sequence, and each contained the entire remainder of the *AKR1* coding region, as determined by restriction digestion analysis (not shown). The interaction observed was due to the *AKR1* sequence and not to sequences elsewhere on the plasmid insert, as shown by transferring only the *AKR1* sequence (from the clone starting at codon 22) into pBTM116,

TABLE 2. Two-hybrid interactions involving *AKR1*, *STE4* ($\text{G}\beta$), *STE18* ($\text{G}\gamma$), and *GPA1* ($\text{G}\alpha$)

Identification no.	Tester cells ^a	Fusion		β -Galactosidase activity ^d
		AD ^b	DBD ^c	
1	Haploid	<i>AKR1</i>	<i>STE18</i>	90 \pm 52
2	Haploid <i>ste4</i> Δ	<i>AKR1</i>	<i>STE18</i>	4.4 \pm 1.4
3	Diploid	<i>AKR1</i>	<i>STE18</i>	1.8 \pm 0.30
4	Haploid	Vector	<i>STE18</i>	0.15 \pm 0.11
5	Haploid	Vector	<i>STE4</i> ^e	0.22 \pm 0.12
6	Haploid	<i>AKR1</i>	<i>STE4</i> ^e	62 \pm 36
7	Haploid	<i>STE4</i>	<i>AKR1</i>	230 \pm 12
8	Diploid	<i>STE4</i>	<i>AKR1</i>	0.16 \pm 0.12
9	Diploid + pSTE18	<i>STE4</i>	<i>AKR1</i>	98 \pm 9.5
10	Haploid	<i>ste4</i> ^{vid}	<i>AKR1</i>	0.41 \pm 0.15
11	Haploid	<i>ste4</i> ^{vid}	<i>STE18</i>	0.13 \pm 0.041
12	Haploid	<i>ste4</i> ^{vid}	<i>GPA1</i>	320 \pm 120
13	Haploid	<i>ste4</i> ^{aid}	<i>AKR1</i>	260 \pm 100
14	Haploid	<i>ste4</i> ^{aid}	<i>STE18</i>	4.0 \pm 1.6
15	Haploid	<i>ste4</i> ^{aid}	<i>GPA1</i>	0.48 \pm 0.029
16	Haploid	<i>STE4</i>	<i>GPA1</i>	370 \pm 14
17	Haploid	<i>STE4</i>	<i>STE18</i>	5.8 \pm 3.5
18	Diploid	<i>STE4</i>	<i>GPA1</i>	160 \pm 26
19	Haploid	Vector	<i>GPA1</i>	0.24 \pm 0.12
20	Haploid	<i>AKR1</i>	<i>GPA1</i>	0.22 \pm 0.14
21	Haploid	<i>AKR1</i>	<i>AKR1</i>	68 \pm 37
22	Haploid	Vector	<i>AKR1</i>	0.13 \pm 0.074

^a The haploid tester is L40; the diploid tester is PPY429; the haploid *ste4* Δ tester is PPY665; pSTE18 is pM70-ADE2, which expresses *STE18* from an *ADH* promoter.

^b Plasmids used are p80.Aw3-1 (*AKR1*), pGAD424 (vector), pGAD-*STE4*, pGm3-F30 (*ste4*^{vid}), and pGm3-E41 (*ste4*^{aid}). *ste4*^{vid} and *ste4*^{aid} indicate mutant derivatives of Ste4p that are defective in the ability to interact with Ste18p ($\text{G}\gamma$) and Gpa1p ($\text{G}\alpha$), respectively (59).

^c Plasmids are pBTM-*STE18*, pB1a (*STE4*), pBTM-*AKR1*, and pBTM-*GPA1*.

^d Expressed in Miller units (54), multiplied by 10 to facilitate comparison. Each value represents the mean \pm standard deviation for three independent transformants.

^e The DBD-*STE4* fusion (plasmid pB1a) is carried on a low-copy-number (CEN) plasmid, whereas all other DBD fusions are carried on high-copy-number (2- μm) plasmids.

creating a fusion with the *lexA* DBD; this derivative showed a positive interaction with an AD-*STE4* fusion (Table 2). The specificity of the Ste4p-Akr1p interaction was addressed initially as follows: Akr1p did not interact with *lexA* DBD fusions to lamin C or Cdc31p, and Ste4p did not interact with *lexA* DBD fusions to lamin C or Cdc31p, with either of three randomly picked fusions from the AD library, or with itself (not shown). Further information about the specificity of the interaction came from more detailed analyses (see below). Interestingly, Akr1p did show an interaction with itself (Table 2, strain 21), raising the possibility that it exists as a multimer in the cell.

The *AKR1* gene was originally identified (42) as displaying a synthetic lethal interaction with the polarity establishment gene *BEM1*. Its coding sequence (42) predicts a protein of 764 amino acids with six ankyrin repeats (7, 53) in the amino-terminal third. Otherwise, the sequence does not lead to any obvious predictions of function. All of the AD-*AKR1* fusions that we identified as interacting with Ste4p include the ankyrin repeats and all sequences C terminal to them.

During the preparation of this report, other groups reported two-hybrid interactions between Ste4p and three other proteins that were not recovered in our screen: Ste5p, Cdc24p, and Syg1p (74, 88, 90). Possible explanations for why these proteins were not found include (i) a requirement for a very specific

protein fragment in order for an interaction to be detectable (see reference 88); (ii) the necessary elimination, in our screen, of clones that caused pheromone resistance (see Materials and Methods and references 74 and 88); and (iii) a requirement for a particular arrangement of fusion constructs—for example, while we have reproduced the reported (90) interaction between DBD-*CDC24* and AD-*STE4* fusions, we cannot detect an interaction between DBD-*STE4* and AD-*CDC24* fusions (59), which would be required in our screen.

Akr1p binds the free G β γ complex. Several observations (Table 2) argue that Akrlp binds preferentially to the G β γ complex rather than to just the G β or G γ subunits alone. First, Akrlp displayed positive interactions with either Ste4p (G β) or Ste18p (G γ) (strains 1, 6, and 7). Second, the interaction observed between Akrlp and either G β or G γ was dependent on the presence of the other member of the G β γ complex, as evidenced by (i) the loss of interaction in α/α diploid cells (strains 3 and 8), which do not express G β or G γ (76); (ii) the rescue of the interaction between G β and Akrlp in diploid cells upon expression of G γ from a promoter that operates in diploids (strain 9); and (iii) the loss of interaction between G γ and Akrlp in haploid cells when the gene encoding G β (*STE4*) was deleted (strain 2). Third, a mutant derivative of G β that cannot bind to G γ (but can still bind to G α) showed loss of binding to Akrlp (strains 10 to 12), arguing that the interaction with Akrlp requires not only the presence of both G β and G γ but their ability to form a heterodimeric G β γ complex.

It is unlikely that the stronger interaction signal of Akrlp with G β γ than G β or G γ alone is due to stabilization of G β by G γ or vice versa, as has been observed for mammalian G β γ complexes (34, 72), because (i) unlike its interaction with Akrlp, interaction of G β (Ste4p) with G α (Gpa1p) is still strong even in the absence of G γ (in diploid cells [strain 18]; see also reference 19) or when G β is defective for binding to G γ (strain 12; see also reference 19); and (ii) immunoblot detection of Ste4p and Ste18p two-hybrid fusions similar to those used here show that expression levels of G β or G γ are not dependent on the presence of the other (19).

A weak interaction between Akrlp and G γ alone was, in fact, detectable (in diploid cells or in *ste4* Δ haploid cells; compare strains 2, 3, with 4 in Table 2), but it was greatly strengthened by the presence of G β (strain 1). This finding suggests that Akrlp may contact G γ and that G β and G γ may bind cooperatively to Akrlp. An analogous interaction between Akrlp and G β alone was not detected (compare strains 8 and 22), but the expression levels of G β and G γ in these constructs are not comparable (not shown; see reference 49).

While it is possible that the interaction between the G β γ complex and Akrlp is indirect, i.e., via another component that bridges between them, we can rule out the involvement of components that are haploid specific, including the pheromone receptors, Gpa1p, and Ste5p (76), since we could detect an interaction in diploids between G β and Akrlp as long as we also provided G γ (Table 2, strain 9). Proof of a direct interaction awaits reconstitution *in vitro* with purified proteins.

A further observation suggests that Akrlp may interact only with the free G β γ complex and not with the G α β γ heterotrimer. To examine the effect of overexpressing G α on the G β γ -Akr1p interaction, it was necessary to delete from the tester strain the *URA3*-marked *lexAop-lacZ* reporter, since our G α -expressing plasmids were also marked with *URA3*. Therefore, we monitored the two-hybrid interaction by the activity of the *lexAop-HIS3* reporter (Fig. 1). The interaction observed between G β γ and Akrlp (specifically, between AD-*STE4* and DBD-*AKR1*) was severely inhibited by overexpression of G α (*GPA1* [Fig. 1, first row]). We suggest that this effect is caused

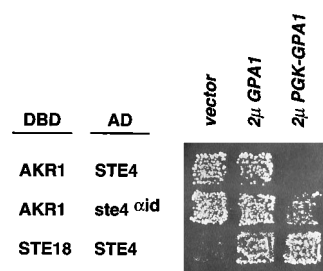


FIG. 1. Overexpression of G α interferes with the G β γ -Akr1p interaction. Cells of strain PPY667 that had been transformed with the indicated combination of DBD fusion and AD fusion plasmids were additionally transformed with a *URA3* 2 μ m plasmid carrying only vector sequence (vector; plasmid YEp24) or the *GPA1* gene (encoding G α) expressed from its own promoter (2 μ *GPA1*; plasmid pG1301) or from the *PGK* promoter (2 μ *PGK-GPA1*; plasmid pPGK-SCG1). Interaction between the DBD and AD fusions caused transcriptional induction of the *lexAop-HIS3* reporter, allowing growth in the absence of histidine, which was measured while maintaining the selection for the *URA3* plasmid (on SC plates lacking histidine and uracil; shown is growth after 5 days at 30°C). Inhibition of the G β γ -Akr1p interaction by high levels of G α is indicated by the loss of growth at the top right. The AD-*ste4*^{oxid} fusion (plasmid pGADm3-D10), whose interaction with the DBD-*AKR1* fusion shows resistance to high levels of G α , encodes a mutant G β that is defective for the ability to bind to G α (59). Similar resistance was observed for three other AD-*ste4*^{oxid} alleles (not shown), including the *ste4*^{Hpl 21-3} allele (85); the one shown here gave the strongest resistance. The signal resulting from the DBD-*STE18*-AD-*STE4* interaction is increased in the presence of the *GPA1* plasmids, presumably because the extra *GPA1* product relieves the selection pressure against accumulation of high copy numbers of *STE18* and *STE4* plasmids, which might otherwise interfere with cell growth by activation of the pheromone response pathway, leading to cell cycle arrest. All results shown here were obtained for at least four independent cotransformants of each combination (not shown).

by driving G β γ into the G α β γ heterotrimer. To observe this inhibition, it was necessary to express *GPA1* from a strong promoter (the *PGK* promoter) on a high-copy-number plasmid; high-copy-number *GPA1* expressed from its own promoter was not sufficient. As controls, (i) mutant derivatives of G β that are defective at binding G α showed binding to Akrlp that was resistant to the inhibitory effect of *GPA1* overexpression (Fig. 1, second row), arguing that the effect of *GPA1* overexpression is directly related to its binding of G β γ , and (ii) interaction between G β and G γ was not inhibited by *GPA1* overexpression (Fig. 1, third row) (in fact, it became easier to detect [see the legend to Fig. 1]), arguing that G α does not inhibit the interaction between G β γ and Akrlp by sequestering G β into a cellular compartment other than the nucleus, where these interactions are measured.

Finally, we did not detect any interaction between Akrlp and G α (Table 2, strain 20), and formation of a G α β γ heterotrimer is not required for interaction with Akrlp, since G β γ bound Akrlp in the absence of G α (in diploid cells [strain 9]) and a mutant version of G β that cannot bind G α (but can still bind G γ) retained its ability to bind to Akrlp (strains 13 to 15). Combining these results with the foregoing observations, therefore, we suggest that Akrlp binds to the free G β γ complex and not to the G α β γ heterotrimer.

Cells lacking Akrlp show defects in growth and cell shape. To investigate further the function of Akrlp, we created a gene deletion by using a construct in which codons 73 through 560 of the 764-amino-acid coding region of *AKR1* were replaced by the *URA3* gene. Upon sporulation of a heterozygous diploid, we found that *akr1::URA3* segregants grew more slowly than their *AKR1* counterparts (Fig. 2). The effect of this growth defect was a roughly twofold-longer doubling time for *akr1* Δ than for *AKR1* in SC medium at 30°C (not shown). In addition, *akr1* Δ cells grew even more slowly at 36 than at 30°C (not

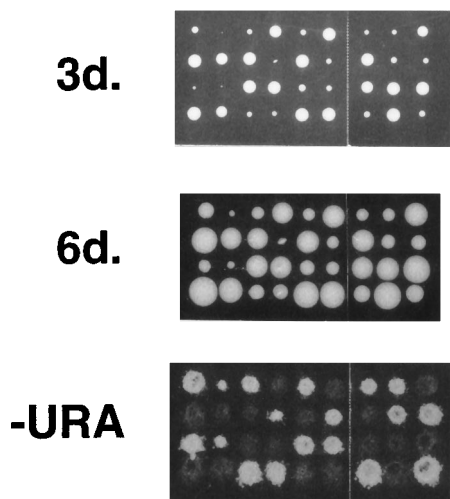


FIG. 2. Cosegregation of the *akr1::URA3* deletion and slow growth. The heterozygous *akr1Δ/AKR1* diploid strain PPY583 was sporulated, and spores were allowed to germinate on YPD; shown are the sizes of the resulting colonies after 3 or 6 days (3d. or 6d.) at 30°C. The colonies were then replicated to SC medium lacking uracil (-URA), upon which only the *akr1::URA3* segregants can grow.

shown) and more slowly on rich medium (YPD) than on SC medium (not shown). The growth defect due to deletion of *AKR1* was seen in each of four different strain backgrounds examined: 381G, A364A, S288C, and W303 (Fig. 3a). How-

ever, we noticed that the severity of the phenotype showed a strong dependence on strain background, especially for the morphological defects described below. We focused our studies on the phenotypes in the 381G background except when it was important to consider other backgrounds (see below).

Morphological examination of the *akr1Δ* cells (Fig. 4a, b, g, and h) revealed a heterogeneous mixture of cell shapes, with some cells appearing relatively normal but many having buds or projections that were elongated, branched, or curved; the less severely affected cells were generally irregular and not as spherical as *AKR1* cells. The cells with severely abnormal morphology were not dead, as judged by their capacity to exclude methylene blue (not shown). Occasionally, groups of abnormal cells appeared connected even after sonication (Fig. 4b and c), suggesting that cytokinesis or cell wall dissolution may be impaired in some fraction of the *akr1Δ* cells. These morphological defects bear some resemblance to those observed in cells deficient in the function of various type 2A phosphatase subunits (6, 32, 66, 84) or the protein kinase Cla4p (22) and in cells hyperactive for the function of the GTPase Cdc42p (92).

Finally, the *akr1Δ* cells rapidly lost viability upon reaching stationary phase (Fig. 5), at a rate of roughly 18% loss per day at 30°C, such that only 9.4% of the *akr1Δ* cells were viable after 12 days, in contrast with essentially 100% of the *AKR1* cells. It appeared that the *akr1Δ* cells were actually dying, rather than failing to resume growth from stationary phase, because the fraction of cells that failed to exclude methylene blue gradually increased during time in stationary phase (not shown). Notably, the less severely abnormal cells in the *akr1Δ* population appeared to die as rapidly as the extremely abnormal cells (as

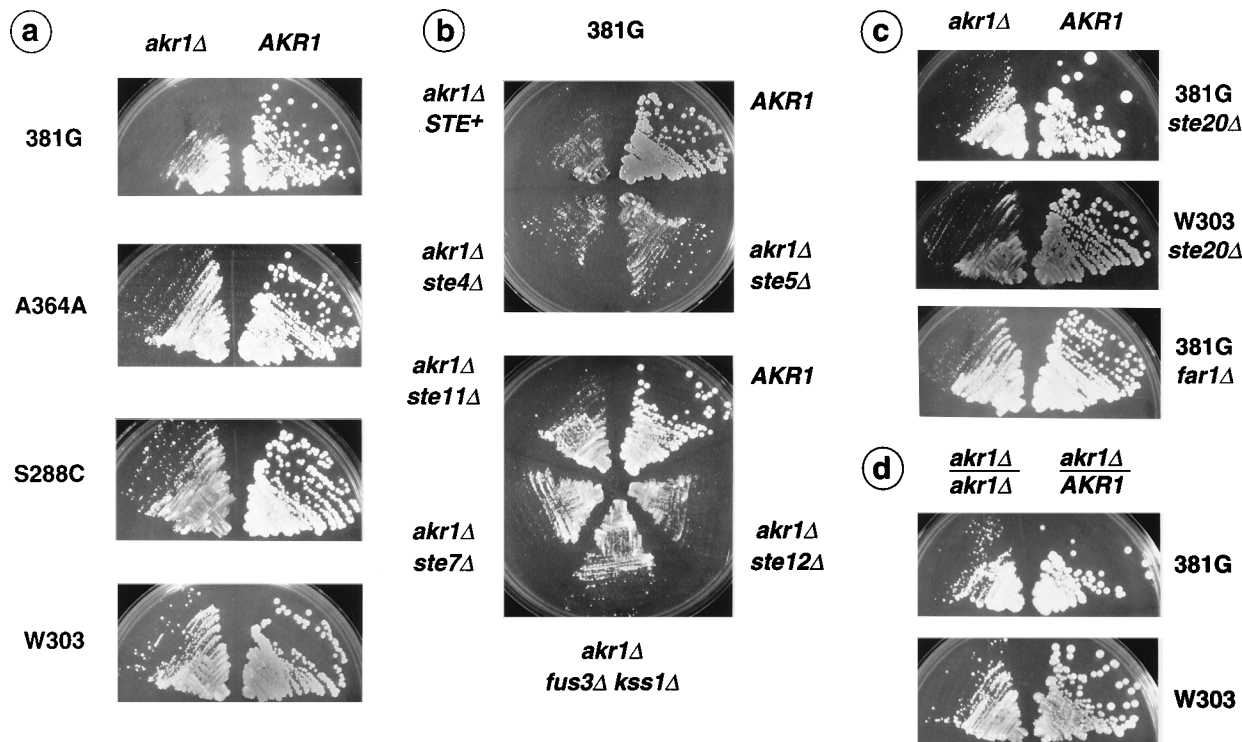


FIG. 3. Comparison of growth rates of *AKR1* and *akr1Δ* cells in various backgrounds and double-mutant combinations. Cells were streaked onto YPD plates and allowed to grow for 2 to 4 days at 30°C, with the exception of the W303 *ste20Δ* strains (panel c), for which growth was at 36°C. (a) 381G strains were PPY618 and PPY617; A364A strains were PPY529 and PPY189; S288C strains were PPY536 and PPY201; W303 strains were PPY553 and PPY495. (b) All strains were in the 381G background. Strains were PPY433, PPY506, PPY510, and PPY512 (top panel) or PPY497, PPY547, PPY516, PPY543, and PPY670 (bottom panel). (c) 381G *ste20Δ* strains were PPY541 and PPY499; W303 *ste20Δ* strains were PPY557 and PPY496; 381G *far1Δ* strains were PPY620 and PPY619. (d) 381G strains were PPY584 and PPY583; W303 strains were PPY651 and PPY653.

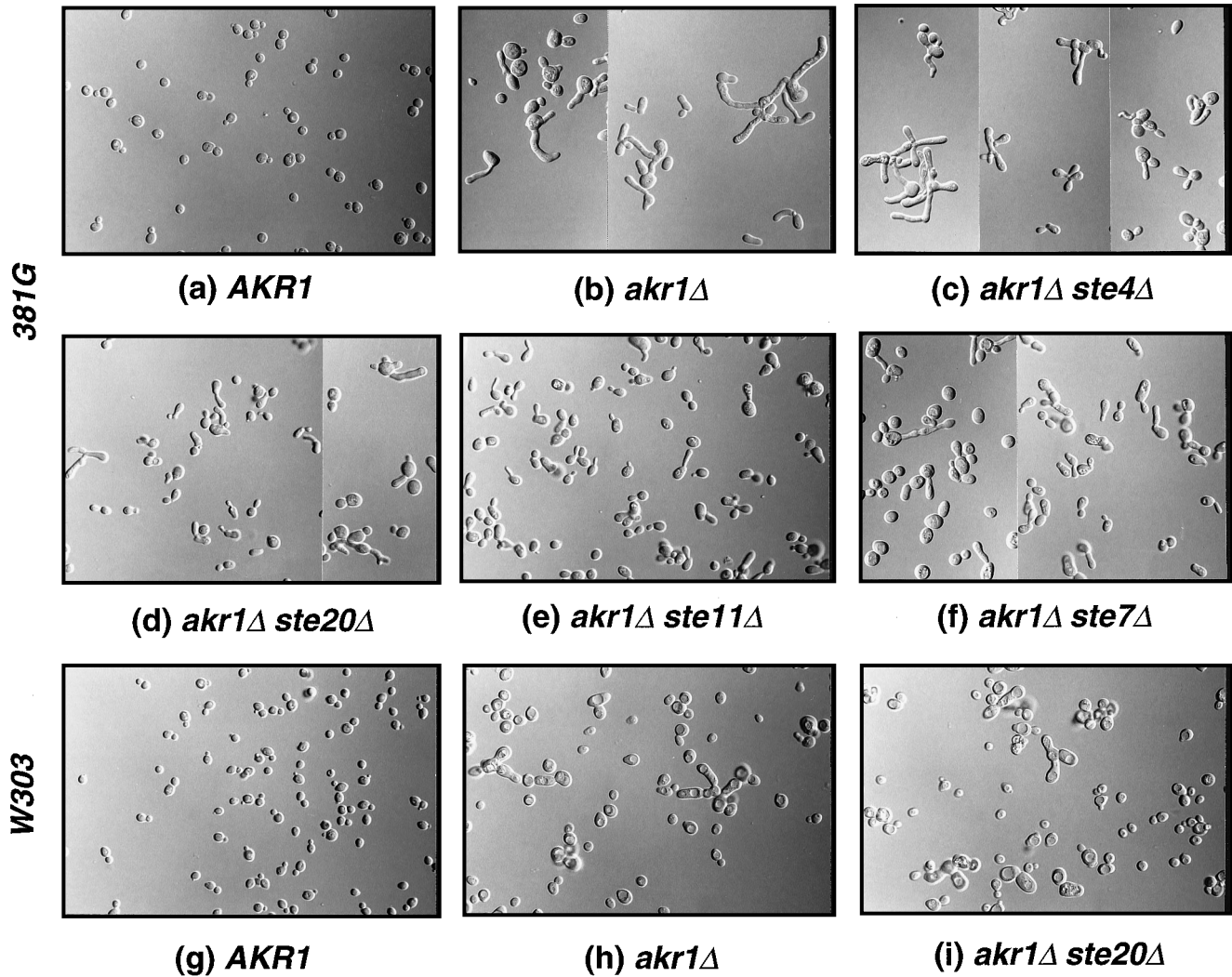


FIG. 4. Morphology of cells lacking Akrlp. Cells were grown and prepared as described in Materials and Methods. Strains: (a) PPY433; (b) PPY506; (c) PPY510; (d) PPY541; (e) PPY547; (f) PPY516; (g) PPY495; (h) PPY553; (i) PPY557.

assayed by dye exclusion [not shown]). It is possible that some fraction of cells in the *akr1Δ* population is always dying even during exponential growth but that loss of these cells is overshadowed by the remainder that are alive and dividing. If this is so, then the loss of viability that we observe would not be specific to stationary phase, but instead the halting of division during stationary phase would simply allow the rate of death to be observed.

Akr1p has a negative effect on the pheromone response pathway. Since Akrlp interacts with a component of the mating response pathway, $G\beta\gamma$, we tested for mating and signalling phenotypes in *akr1Δ* mutants. Cells with a deletion of *AKR1* did not show an appreciable mating defect (83% of *AKR1* efficiency). The frequency of mating to pheromoneless cells in a mating partner discrimination assay (37), which measures the ability of cells to properly determine the source of pheromone, was increased 43-fold over that in *AKR1* cells (from 9.3×10^{-6} to 4.0×10^{-4}); while this defect is roughly similar in strength to that observed for myosin, actin, and clathrin mutants (39), we consider it to be relatively mild since 99.96% of the *akr1Δ* cells that mated still appropriately chose to mate to the pheromone-producing cells.

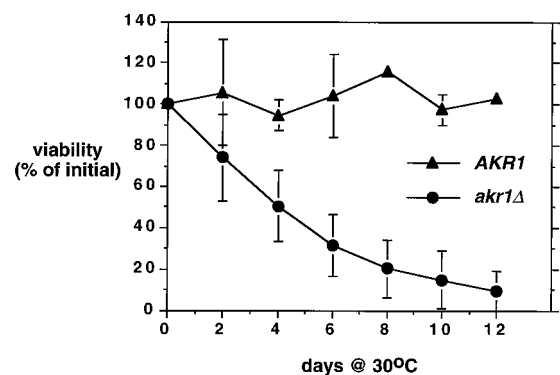


FIG. 5. Loss of viability of *akr1Δ* cells in stationary phase. Cell cultures were grown to stationary phase in SC liquid medium at 30°C and were allowed to continue incubation with agitation for an additional 12 days. Aliquots were removed every 2 days, and appropriate dilutions were plated onto SC plates to measure the number of viable cells remaining. The percentage of the initial CFU is given. Shown are the means \pm ranges of duplicate samples for *AKR1* and the means \pm standard deviations for six parallel samples for *akr1Δ*; viability for the *akr1Δ* cultures after 12 days ranged from 0.26 to 20% of the initial level. Strains were PPY433 (*AKR1*) and PPY506 (*akr1Δ*).

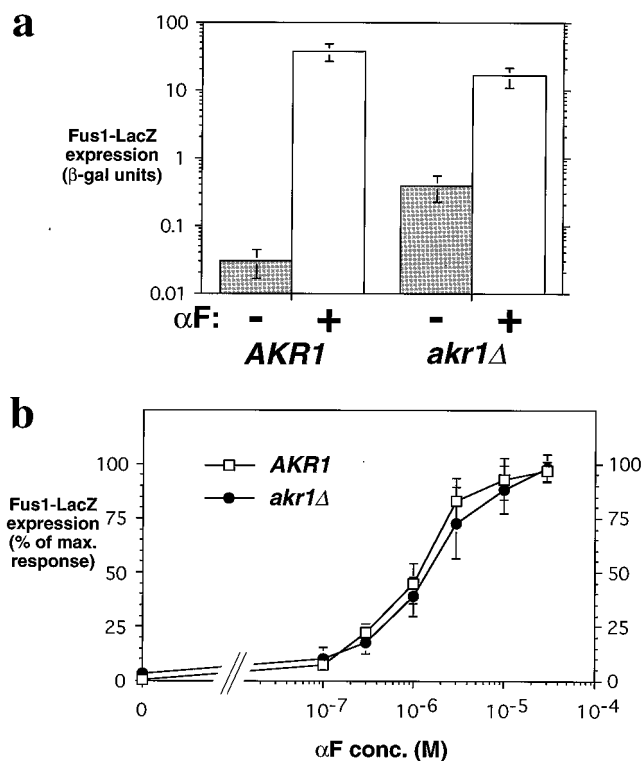


FIG. 6. Effect of *akr1Δ* on signalling through the pheromone response pathway. The level of β -galactosidase (β -gal) activity expressed from a pheromone-inducible Fus1-LacZ construct was measured for *AKR1* and *akr1Δ* cells. (a) Comparison of basal and induced levels of signalling. Activity was measured both in the absence and in the presence of a saturating concentration of pheromone (α F; 3×10^{-5} M). Values shown are means \pm standard deviations for samples assayed in triplicate from three independent experiments. Strains were PPY433 (*AKR1*) and PPY506 (*akr1Δ*). (b) Dose-response profile. Cells were exposed to the indicated concentrations of pheromone for 90 to 135 min before measurement of β -galactosidase activity. Fus1-LacZ expression is plotted as the percentage of the maximum response for each strain; the actual average β -galactosidase activities at the highest concentration of pheromone (3×10^{-5} M) were 36 ± 11 U (*AKR1*) and 16 ± 5.5 U (*akr1Δ*). Other congenic pairs of *AKR1* and *akr1Δ* strains show induced levels of Fus1-LacZ activity in *akr1Δ* mutants that are equal to or even slightly higher than those in *AKR1* controls. Values shown are means \pm standard deviations from three independent experiments, each of which was performed in triplicate. Strains were PPY433 (*AKR1*) and PPY506 (*akr1Δ*).

We checked the activity of the pheromone response pathway in *akr1Δ* cells by monitoring the level of a pheromone-responsive Fus1-LacZ reporter construct, both in the presence and in the absence of pheromone. We found that the basal, uninduced level of Fus1-LacZ expression was elevated in *akr1Δ* mutants, on average 13-fold (Fig. 6a). Thus, the *AKR1* gene product appears to have a negative influence on some component of this signalling pathway. Nevertheless, the addition of saturating concentrations of pheromone could further induce Fus1-LacZ transcription an additional 40-fold (Fig. 6a); therefore, in the absence of pheromone, the signalling pathway in *akr1Δ* mutants is activated to 2.5% of the maximum level (or up to 10% in some strains [not shown]). Dose-response experiments (Fig. 6b) show that although *akr1Δ* cells have a partially activated pheromone response pathway, they are not supersensitive to pheromone, since the concentration of pheromone required to give 50% maximal pheromone response was essentially the same for *akr1Δ* and *AKR1* cells; this observation differs from results with some other genes that negatively regulate the pheromone response pathway, such as *SST2* (10).

The *akr1Δ* cells were still susceptible to growth arrest by pheromone (not shown), as determined by halo assays (75).

The negative effect of Akr1p is on the kinase cascade, not on G β γ . The increased signalling through the pheromone response pathway seen in cells deleted for *AKR1*, coupled with the observation that Akr1p binds to G β γ , initially suggested to us that Akr1p might negatively regulate the activity of G β γ . To address this suggestion, we combined deletion of *AKR1* with deletion of known components of the pheromone response pathway and assayed each double mutant for its basal Fus1-LacZ activity (Fig. 7). We found that deletion of *STE4*, encoding the G β subunit of the G β γ complex, did not affect the elevated basal signalling seen in *akr1Δ* cells (compare rows 2 and 3). Thus, although Akr1p binds the G β γ complex and has a negative influence on the signalling pathway, it is not simply a negative regulator of G β γ activity, since its effect on signalling is independent of the presence of the G β subunit. Some other examples of elevated basal signalling, due to constitutive activation of the Ste11p kinase or mutation of the *RGAI* gene, have also been found to be independent of the *STE4* product (77, 78).

In contrast to deletion of *STE4*, the elevated basal signalling in *akr1Δ* cells was eliminated by deletions of genes encoding components of the kinase cascade (*STE11* and *STE7*) and the downstream transcription factor (*STE12*). This result suggested that the negative effect of Akr1p on signalling acts on the kinase cascade, at the level of, or upstream of, Ste11p. The only known kinase upstream of Ste11p is encoded by *STE20*. We found that deletion of *STE20* did not eliminate the elevated basal signalling of *akr1Δ* mutants in the 381G background (Fig. 7, middle rows). However, in this strain background, *ste20Δ* cells are not defective for Fus1-LacZ induction in response to pheromone and are only partially defective for mating, not sterile (60). Therefore, we also analyzed an *akr1Δ ste20Δ* double mutant in another strain background, W303, in which deletion of *STE20* causes sterility and a nearly complete loss of Fus1-LacZ induction in response to pheromone (47, 62). In this case, we found that deletion of *STE20* did eliminate the elevated signalling of *akr1Δ* cells (Fig. 7, bottom rows). Thus, we conclude that deletion of *AKR1* probably leads to activation of Ste20p in both strain backgrounds but that Ste20p is redundant with another function in the 381G background.

Finally, deletion of *STE5* did not eliminate the elevated basal signalling in *akr1Δ* cells, but it did lower it (Fig. 7, fourth row). This observation parallels one made with constitutively activated Ste11p mutants, in which signalling *in vivo* by this kinase was still active in *ste5Δ* cells but was partially reduced (78). Therefore, we feel that our observation is consistent with the view that the kinase cascade becomes partially activated in cells lacking Akr1p.

Growth and morphological effects of *AKR1* are separable from signalling. Since activation of the pheromone response pathway causes both arrest of the cell cycle and changes in cell shape, we asked whether the growth and morphological phenotypes of *akr1Δ* cells are the result of the increased signalling through the pathway. Therefore, using the *akr1Δ steΔ* double mutants described above, we compared those that did and did not have elevated signalling for their growth and morphological properties. Importantly, neither those deletions that did eliminate the elevated basal signalling of *akr1Δ* cells (*ste20Δ*, *ste11Δ*, *ste7Δ*, and *ste12Δ*) nor deletion of a gene required for cell cycle arrest (*FAR1*) could rescue the slow growth of *akr1Δ* cells or return their morphology to normal (Fig. 3b and c and 4; summarized in Fig. 7). In addition, none of these deletions could rescue the death of *akr1Δ* cells observed in stationary phase (as assayed by dye exclusion [not shown]). These data

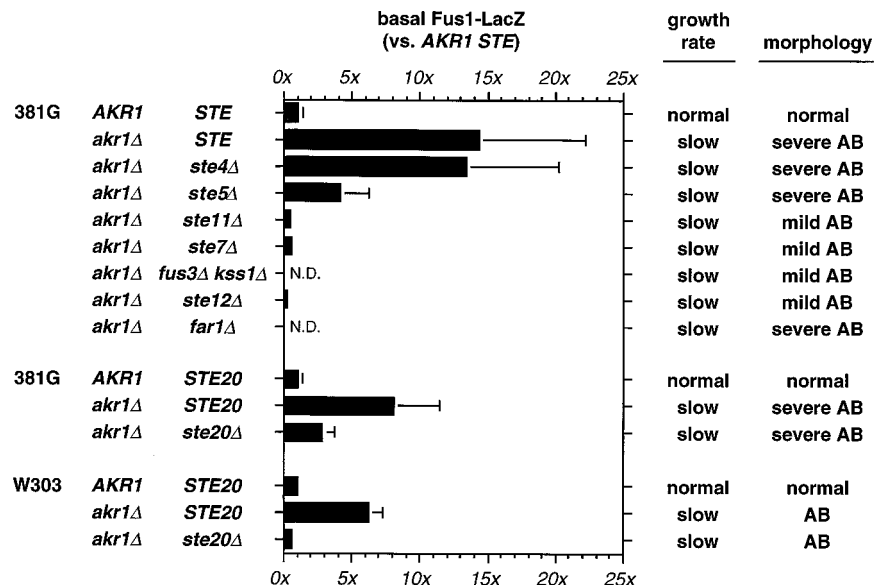


FIG. 7. Epistasis analysis of *akr1Δ steΔ* double mutants. Cells of the indicated genotypes were assayed for basal Fus1-LacZ activity, growth rate, and cellular morphology. Values for basal Fus1-LacZ activity are shown relative to that for the congenic wild-type (*AKR1 STE*) control strain (=1×); shown are the means ± standard deviations of 4 to 21 separate measurements of each strain. For each strain indicated, similar results were obtained for two or three additional isogenic strains (not shown). The growth and morphological properties of each strain are summarized at the right, and the data for all (growth) or examples (morphology) are shown in Fig. 3 and 4. Strains used were as follows: top set (from top to bottom), PPY433, PPY506, PPY510, PPY512, PPY547, PPY516, PPY543, PPY670, and PPY620; middle set (from top to bottom), PPY600, PPY603, and PPY541; bottom set (from top to bottom), PPY646, PPY647, and PPY648. AB, abnormal; N.D., not determined.

demonstrate that the slow growth of *akr1Δ* cells is not caused by activation of the cell cycle arrest pathway and that their abnormal morphology is not caused by activation of the kinase cascade or increased transcription of pheromone-inducible genes. Therefore, the slow growth and abnormal morphology of *akr1Δ* mutants cannot be attributed to hyperactivity of any one of the known positive components of the pheromone response pathway. It should be noted, however, that the severity of the morphological phenotype showed a dependence on whether the signalling pathway leading to elevated Fus1-LacZ activity was intact: the morphological phenotype was most severe for *STE*⁺, *ste4Δ*, and *ste5Δ* and was less severe (but still noticeable) for *ste11Δ*, *ste7Δ*, *fus3Δ kss1Δ*, and *ste12Δ* (compare Fig. 4b and c with Fig. 4e and f) (summarized in Fig. 7). Thus, it appears that deletion of *AKR1* causes morphological abnormalities that are independent of pheromone response pathway activity but are accentuated by the elevated signalling through the kinase cascade. This accentuation is not surprising, since activation of the lower part of the pheromone response pathway can give rise to at least some morphological changes (23, 78).

Phenotypes of *akr1Δ/akr1Δ* diploids. Loss of *Akr1p* function also had an effect in *a/α* diploid cells. Specifically, the same phenotypes observed in *akr1Δ* haploids were seen in *akr1Δ/akr1Δ* diploids: slow growth (Fig. 3d), abnormal morphology (Fig. 8), and elevated levels of Fus1-LacZ activity (from 10- to 46-fold, with an average of 29- ± 13-fold [*n* = 6], compared with *akr1Δ/AKR1* diploids). Related to this last phenotype, overexpression of the transcription factor *Ste12p* from a galactose-inducible promoter also gave strong Fus1-LacZ induction, even in wild-type *a/α* diploids (not shown). All of these phenotypes observed in *akr1Δ/akr1Δ* diploids are recessive, since *akr1Δ/AKR1* heterozygotes resembled wild-type *AKR1/AKR1* diploids.

Among the morphologies observed in *akr1Δ/akr1Δ* diploids,

a variable fraction of the cells displayed characteristics of the diploid pseudohyphal growth pathway (29, 44), including elongated cells, connected chains of cells, and an arrangement of connected cells suggestive of a unipolar budding pattern (Fig. 8b); unfortunately, heterogeneity of cellular morphologies and strongly delocalized Calcofluor staining (not shown) made it difficult to score the fraction of cells actually executing the unipolar budding pattern. These features were not observed in wild-type or *akr1Δ/AKR1* diploids, which showed the normal bipolar budding pattern. Since components of the pheromone-responsive kinase cascade (*Ste20p*, *Ste11p*, and *Ste7p*) and the downstream transcription factor (*Ste12p*) are required in diploids for transition to pseudohyphal growth (50, 65), this observation reinforces the conclusion presented above that this kinase cascade becomes partially activated in cells lacking *Akr1p*. By analogy with our results in haploids, we would predict that *akr1Δ/akr1Δ* diploids that had further deletions of both copies of the genes encoding components of the kinase cascade or downstream transcription factor (e.g., *ste11Δ/ste11Δ* or *ste12Δ/ste12Δ*) would be rescued only for the elevated Fus1-LacZ phenotype and not for the growth and morphological phenotypes. We have not yet tested this prediction.

Finally, the *akr1Δ/akr1Δ* diploids also displayed strong defects in sporulation (not shown), which could be an indirect consequence of poor growth or abnormal morphology or could be more directly related to aberrant signalling in cells lacking *Akr1p*. We have not yet attempted to distinguish between these possibilities.

DISCUSSION

***Akr1p* binds Gβγ and has an influence on both cell morphology and signalling.** We are interested in how the yeast pheromone response pathway communicates with components that govern cell shape and polarity. On the basis of studies of

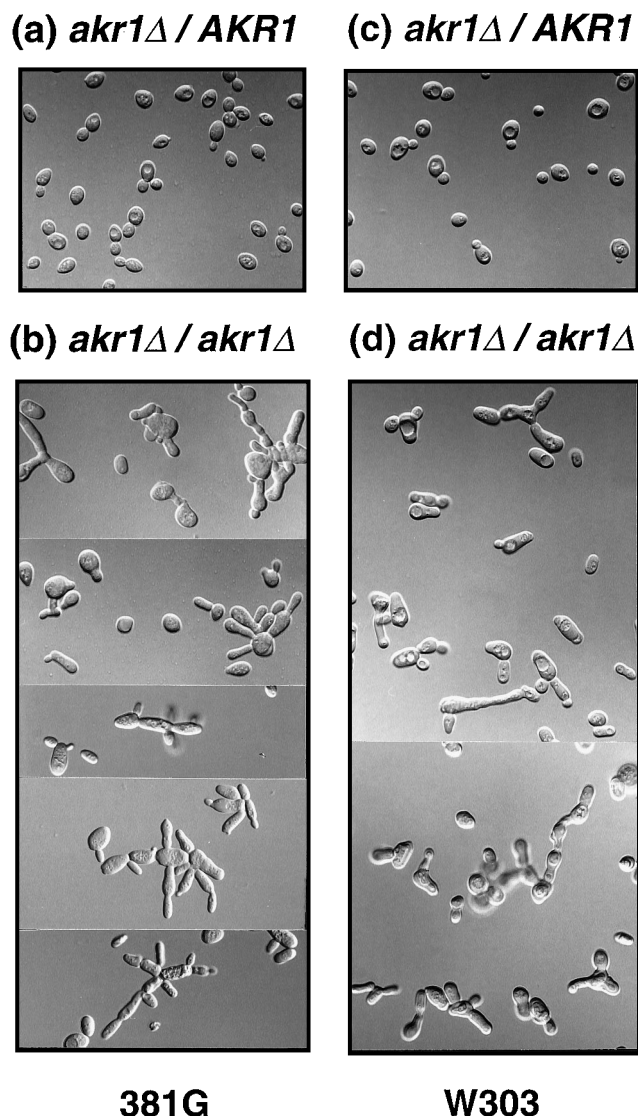


FIG. 8. Morphology of diploid cells lacking Akrlp. Cells were grown and prepared as described in Materials and Methods. Diploids homozygous for deletion of *AKR1* show a tendency toward morphological features characteristic of pseudohyphal growth (see text). In some cases, multiple buds arising from a single pole project above or below the plane of focus. Strains: (a) PPY583; (b) PPY584; (c) PPY653; (d) PPY651.

the ability of yeast cells to polarize toward mating partners producing pheromone, we had reason to believe that either the pheromone receptor, the $G\alpha$ subunit of the receptor-coupled G protein, or the $G\beta\gamma$ complex was responsible for interacting with determinants of cell shape and polarity (67). Because it has been difficult by genetic analysis to distinguish between these possible candidates, we decided to search directly for gene products that bind to each of them.

We began our search with the $G\beta\gamma$ complex and had anticipated two distinct effectors for $G\beta\gamma$: one for its known function in activating the signal transduction pathway, and one for its hypothetical function in communicating with determinants of cell shape and polarity. Instead, we found only one gene, *AKR1*, whose product interacts with $G\beta\gamma$ but which when deleted has effects on both signalling and cell shape. Thus, via Akrlp, $G\beta\gamma$ may indeed participate in the control of cell shape

and polarity in addition to carrying out its known function in signalling, but these functions may be less distinct than suggested by our simplest initial hypothesis (see below). Importantly, the effect of deleting *AKR1* on cell shape is not caused by the increased signalling, since it was not eliminated by deletion of any of the pheromone response genes, even though the signalling was eliminated by some deletions (Fig. 7). This observation leads us to consider that the morphological defect in *akr1Δ* cells may cause the increased signalling, rather than vice versa (see below).

How does $G\beta\gamma$ activate the downstream pathway? While recent biochemical evidence has solidified our understanding of signal transmission through the pheromone-responsive kinase cascade (24, 26, 56, 89, 91), the mechanism by which this kinase cascade is activated by the free $G\beta\gamma$ complex remains unclear. It is possible that $G\beta\gamma$ directly activates the next genetically defined component, which could be either Ste5p or Ste20p (31, 47, 62), or, alternatively, there may be additional intermediates in this pathway, as has been suggested recently (see below). It is notable that recent work in a mammalian cell system suggests that at least five intermediate components are required for the activation of a mitogen-activated protein kinase cascade by a $G\beta\gamma$ complex (81, 83).

What is the direct target of $G\beta\gamma$ activity in yeast cells? During the preparation of the manuscript, reports from three other groups suggested that $G\beta\gamma$ interacts with three different proteins: Ste5p, Cdc24p, and Syg1p (74, 88, 90). We show here that $G\beta\gamma$ can interact with a fourth protein, Akrlp. Interestingly, while Akrlp binds to the free $G\beta\gamma$ complex, it appears to be excluded from binding to the $G\alpha\beta\gamma$ heterotrimer (Fig. 1). These are properties expected for an effector of $G\beta\gamma$; namely, pheromone should activate the ability of $G\beta\gamma$ to interact with an effector by releasing $G\beta\gamma$ from the inhibitory $G\alpha$ subunit. Surprisingly for a candidate effector, however, Akrlp has a negative influence on the signal transduction pathway. Thus, if Akrlp is an effector of $G\beta\gamma$, the role of the $G\beta\gamma$ -Akrlp interaction might be to antagonize the negative effect of Akrlp on downstream events (Fig. 9). Consistent with this view, the negative effect of Akrlp on signalling acts on the kinase cascade downstream of $G\beta\gamma$ and not on $G\beta\gamma$ itself (Fig. 7).

While Akrlp could affect the kinase cascade directly, it could also act indirectly, by negatively regulating the activities of intermediates that participate in the transfer of signal from $G\beta\gamma$ to the downstream kinase cascade. There are three reasons to consider this second possibility. First, *akr1Δ* mutants have abnormal morphology in all *ste* deletions (Fig. 4 and 7), so at least one target of Akrlp, and maybe the primary target, still functions abnormally in these double mutants. Second, mutations in *AKR1* display synthetic lethality with mutations in *BEM1* (42), suggesting that Akrlp function relates to the activities of the polarity establishment gene products. Third, recent evidence suggests that the proteins Bem1p, Cdc24p, and Cdc42p, which are required for the control of cell shape and polarity (1, 40, 73), are also involved in pheromone-responsive signalling (42, 71, 77, 90), and GTP-bound Cdc42p can stimulate the kinase activity of the first kinase in the pheromone-responsive kinase cascade, Ste20p (71). Since $G\beta\gamma$ interacts with both Ste5p (88) and Cdc24p (90), perhaps it activates the pathway by bridging together two multiprotein complexes—one consisting of Ste5p and its associated kinases Ste11p, Ste7p, and Fus3/Kss1p, and the other consisting of Bem1p, Cdc24p, Cdc42p, and the kinase Ste20p—to thereby promote phosphorylation of Ste11p by Ste20p.

A model for Akrlp function. Consolidating the foregoing observations, we suggest a model in which Akrlp participates in the activation by the free $G\beta\gamma$ complex of both the down-

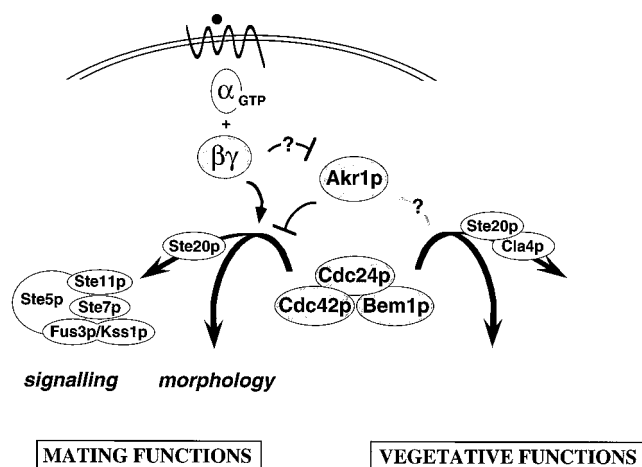


FIG. 9. Model for Akrl1p function. Akrl1p is proposed to control the function of Bem1p, Cdc24p, and/or Cdc42p by preventing them from activating targets involved in mating, including the pheromone-responsive kinase cascade, until G $\beta\gamma$ is activated by pheromone. Activation of targets involved in vegetative growth may also be inhibited by Akrl1p or may be in effect promoted by inhibited access to mating targets. There are likely to be direct mechanisms for activation of downstream signalling components by G $\beta\gamma$. The net effect is that G $\beta\gamma$ instructs the polarity establishment gene products to activate pathways contributing to signalling (through the kinase cascade) and cell morphology. Akrl1p may help G $\beta\gamma$ control a switch in targets of the polarity establishment gene products. See text for additional details.

stream kinase cascade and the determinants of cell shape and polarity (Fig. 9). In this model, Akrl1p serves to inhibit the activity of one or more of the polarity establishment gene products, Bem1p, Cdc24p, and Cdc42p. This inhibition could be direct or indirect (such as by blocking access to a target or restricting their spatial localization) and could affect all functions of these proteins or only functions specific to mating. The free G $\beta\gamma$ complex, liberated from G α in response to pheromone, is responsible for activating the polarity establishment gene products, which would then activate both the kinase cascade and unknown targets responsible for changes in cell shape. The interaction between G $\beta\gamma$ and Akrl1p may serve as a prerequisite step in order to antagonize the negative effect of Akrl1p or for G $\beta\gamma$ to gain access to the polarity establishment gene products.

We suggest that the phenotypes of cells deleted for *AKR1* are the result of inappropriate (increased, unregulated, or improperly localized) activity of the polarity establishment proteins, and, ultimately, of the GTPase Cdc42p. This supposition explains why the slow growth and abnormal morphology of *akr1* Δ cells are not rescued by deletion of pheromone response pathway components, even though the signalling phenotype can be relieved (Fig. 7). Presumably, Cdc42p has targets in addition to the pheromone-responsive kinase cascade, and therefore the activities of these targets would still be aberrant in *akr1* Δ cells even when the signalling phenotype is eliminated by deletion of *STE20* or other downstream elements. Likely targets of Cdc42p function now include both Ste20p (71) and its related kinase Cla4p (22), and probably additional proteins involved in actin organization (22), so that even in *akr1* Δ *ste20* Δ double mutants, improper activity of Cla4p and/or other Cdc42p targets might lead to growth and morphological defects. In this regard, it is notable that both elimination of Cla4p function and hyperactivity of Cdc42p cause morphological deformities similar to those in *akr1* Δ mutants (22, 92). In addition, recent evidence suggests that combining deletion of *AKR1* with that of *CLA4* results in lethality or an additive

growth defect with a severely exaggerated morphological and cytokinesis defect, depending on strain background (59).

One facet of our model is that Akrl1p may participate in coupling the activities of a Bem1p-Cdc24p-Cdc42p complex to an upstream signalling system, the pheromone-responsive G protein. Since both this complex and Ste20p must function during vegetative growth (1, 5, 22, 73) without activating the pheromone response pathway, there must be mechanisms to limit their activities to targets appropriate for the process intended, e.g., bud formation or mating. Akrl1p may help G $\beta\gamma$ divert this complex away from targets essential for growth and toward targets involved in mating (Fig. 9). Since Akrl1p is also required in diploid cells, it may interact with signalling systems other than the pheromone-responsive G protein and may assist in preventing cross talk between related but functionally separate signalling systems. In this regard, the activation of *Fus1-LacZ* in *akr1* Δ /*akr1* Δ diploids (see Results) may provide a clue to the defect in cells lacking Akrl1p function. Although elements of the pheromone response pathway are also utilized by haploid agar invasion and diploid pseudohyphal growth pathways (50, 65), *FUS1* is not induced during the agar invasion pathway (65). Thus, either *FUS1* is induced during pseudohyphal growth in diploids or the manner of activation of the kinase cascade in *akr1* Δ /*akr1* Δ diploids is in some way different from the manner in which it is activated during pseudohyphal growth. Perhaps in both haploid and diploid cells deficient in Akrl1p activity, several kinase cascades that are normally activated by distinct stimuli become activated such that the mutant cells are simultaneously attempting mating, agar invasion, and pseudohyphal growth programs. Thus, Akrl1p might functionally segregate different signalling modules, perhaps by multimerization via Akrl1p-Akrl1p interactions (Table 2).

Any model for Akrl1p function must account for the observation that deletion of *AKR1* only partially activates the pheromone response pathway, which can be further activated by G $\beta\gamma$ in response to pheromone in *akr1* Δ cells. In addition, *akr1* Δ mutants show no appreciable defect in mating efficiency or partner choice, and so some mechanisms of control of cell polarity by the pheromone response pathway must still be intact. It is possible that Akrl1p is partially redundant with other proteins. Indeed, a recent two-hybrid screen for proteins that interact with Ste18p (G γ) has yielded not only *AKR1* but also a new gene (whose sequence was recently deposited [GenBank accession number X87331, entry name SPAC2F7.10] that is highly similar to *AKR1* (61) (there is also a *Schizosaccharomyces pombe* homolog of these two [GenBank accession number Z50142, entry name SCXV58KB.25]). Given the recent reports suggesting that G $\beta\gamma$ can interact with both Ste5p and Cdc24p (88, 90), however, it seems likely that there is direct activation of downstream components by G $\beta\gamma$. The role of Akrl1p may be to facilitate this process by preventing premature activation or to allow G $\beta\gamma$ to divert the polarity establishment proteins away from essential targets and toward mating-specific targets. Further work should help to distinguish among these possibilities. Most importantly, our model makes predictions about the role of the interaction between G $\beta\gamma$ and Akrl1p: it predicts that while *akr1* Δ cells are fertile, the ability of G $\beta\gamma$ to interact with Akrl1p may be an important or essential prerequisite to further action by G $\beta\gamma$; thus, disruption of the G $\beta\gamma$ -Akrl1p interaction through mutations in the G $\beta\gamma$ complex or through mutations in Akrl1p (that retain its negative activity) may result in signalling or mating defects. This prediction is currently being tested.

ACKNOWLEDGMENTS

We thank K. Schrick, D. Jenness, H. McDonald, M. Brown, S. Hollenberg, E. Leberer, P. James, and E. Craig for reagents and advice; B. Thornton, B. Margulies, and O. Hubbard for technical assistance; A. Neiman, D. Toczyski, R. Dorer, and B. Thornton for discussion and comments on the manuscript; and A. Bender and G. F. Sprague, Jr., for discussion of results prior to publication.

This work was supported by NIH grant GM61-4590. P.M.P. was supported by fellowship DRG1158 from the Damon Runyon-Walter Winchell Cancer Research Fund. L.H.H. is an American Cancer Society Professor.

REFERENCES

- Adams, A. E., D. I. Johnson, R. M. Longnecker, B. F. Sloat, and J. R. Pringle. 1990. *CDC42* and *CDC43*, two additional genes involved in budding and the establishment of cell polarity in the yeast *Saccharomyces cerevisiae*. *J. Cell Biol.* **111**:131-142.
- Altschul, A. F., W. Gish, W. Miller, E. W. Myers, and D. J. Lipman. 1990. Basic local alignment search tool. *J. Mol. Biol.* **215**:403-410.
- Bardwell, L., J. G. Cook, C. J. Inouye, and J. Thorner. 1994. Signal propagation and regulation in the mating pheromone response pathway of the yeast *Saccharomyces cerevisiae*. *Dev. Biol.* **166**:363-379.
- Bartel, P. L., C. Chien, R. Sternglanz, and S. Fields. 1993. Using the two-hybrid system to detect protein-protein interactions, p. 153-179. *In* D. A. Hartley (ed.), *Cellular interactions in development: a practical approach*. IRL Press, Oxford.
- Bender, A., and J. R. Pringle. 1991. Use of a screen for synthetic lethal and multicopy suppressive mutants to identify two new genes involved in morphogenesis in *Saccharomyces cerevisiae*. *Mol. Cell Biol.* **11**:1295-1305.
- Blacketer, M. J., C. M. Koehler, S. G. Coats, A. M. Myers, and P. Madaule. 1993. Regulation of dimorphism in *Saccharomyces cerevisiae*: involvement of the novel protein kinase homolog Elm1p and protein phosphatase 2A. *Mol. Cell Biol.* **13**:5567-5581.
- Bork, P. 1993. Hundreds of ankyrin-like repeats in functionally diverse proteins: mobile modules that cross phyla horizontally? *Proteins Struct. Funct. Genet.* **17**:363-374.
- Botstein, D., S. C. Falco, S. E. Stewart, M. Brennan, S. Scherer, D. T. Stinchcomb, K. Struhl, and R. W. Davis. 1979. Sterile host yeasts (SHY): a eukaryotic system of biological containment for recombinant DNA experiments. *Gene* **8**:17-24.
- Cadwell, R. C., and G. F. Joyce. 1992. Randomization of genes by PCR mutagenesis. *PCR Methods Appl.* **2**:28-33.
- Chan, R. K., and C. A. Otte. 1982. Physiological characterization of *Saccharomyces cerevisiae* mutants supersensitive to G1 arrest by a factor and α factor pheromones. *Mol. Cell Biol.* **2**:21-29.
- Chang, F., and I. Herskowitz. 1990. Identification of a gene necessary for cell cycle arrest by a negative growth factor of yeast: FAR1 is an inhibitor of a G1 cyclin, CLN2. *Cell* **63**:999-1011.
- Chant, J. 1994. Cell polarity in yeast. *Trends Genet.* **10**:328-333.
- Chant, J., and J. R. Pringle. 1991. Budding and cell polarity in *Saccharomyces cerevisiae*. *Curr. Opin. Genet. Dev.* **1**:342-350.
- Chenevert, J. 1994. Cell polarization directed by extracellular cues in yeast. *Mol. Biol. Cell* **5**:1169-1175.
- Chenevert, J., K. Corrado, A. Bender, J. Pringle, and I. Herskowitz. 1992. A yeast gene (BEM1) necessary for cell polarization whose product contains two SH3 domains. *Nature (London)* **356**:77-79.
- Chenevert, J., N. Valtz, and I. Herskowitz. 1994. Identification of genes required for normal pheromone-induced cell polarization in *Saccharomyces cerevisiae*. *Genetics* **136**:1287-1296.
- Chien, C. T., P. L. Bartel, R. Sternglanz, and S. Fields. 1991. The two-hybrid system: a method to identify and clone genes for proteins that interact with a protein of interest. *Proc. Natl. Acad. Sci. USA* **88**:9578-9582.
- Choi, K. Y., B. Satterberg, D. M. Lyons, and E. A. Elion. 1994. Ste5 tethers multiple protein kinases in the MAP kinase cascade required for mating in *S. cerevisiae*. *Cell* **78**:499-512.
- Clark, K. L., D. Dignard, D. Y. Thomas, and M. Whiteway. 1993. Interactions among the subunits of the G protein involved in *Saccharomyces cerevisiae* mating. *Mol. Cell Biol.* **13**:1-8.
- Cole, G. M., D. E. Stone, and S. I. Reed. 1990. Stoichiometry of G protein subunits affects the *Saccharomyces cerevisiae* mating pheromone signal transduction pathway. *Mol. Cell Biol.* **10**:510-517.
- Cross, F., L. H. Hartwell, C. Jackson, and J. B. Konopka. 1988. Conjugation in *Saccharomyces cerevisiae*. *Annu. Rev. Cell Biol.* **4**:429-457.
- Cvrckova, F., C. DeVirgilio, E. Manser, J. R. Pringle, and K. Nasmyth. 1995. Ste20-like protein kinases are required for normal localization of cell growth and for cytokinesis in budding yeast. *Genes Dev.* **9**:1817-1830.
- Dolan, J. W., and S. Fields. 1990. Overproduction of the yeast STE12 protein leads to constitutive transcriptional induction. *Genes Dev.* **4**:492-502.
- Elion, E. A., B. Satterberg, and J. E. Kranz. 1993. FUS3 phosphorylates multiple components of the mating signal transduction cascade: evidence for STE12 and FAR1. *Mol. Biol. Cell* **4**:495-510.
- Elledge, S. J., J. T. Mulligan, S. W. Ramer, M. Spottswood, and R. W. Davis. 1991. λ YES: a multifunctional cDNA expression vector for the isolation of genes by complementation of yeast and *Escherichia coli* mutations. *Proc. Natl. Acad. Sci. USA* **88**:1731-1735.
- Errede, B., A. Gartner, Z. Zhou, K. Nasmyth, and G. Ammerer. 1993. MAP kinase-related FUS3 from *S. cerevisiae* is activated by STE7 *in vitro*. *Nature (London)* **362**:261-264.
- Field, C., and R. Scheckman. 1980. Localized secretion of acid phosphatase reflects the pattern of cell surface growth in *Saccharomyces cerevisiae*. *J. Cell Biol.* **86**:123-128.
- Gietz, R. D., R. H. Schiestl, A. R. Willems, and R. Woods. 1995. Studies on the transformation of intact yeast cells by the LiAc/SS-DNA/PEG procedure. *Yeast* **11**:355-360.
- Gimeno, C. J., P. O. Ljungdahl, and C. A. Styles. 1992. Unipolar cell divisions in the yeast *S. cerevisiae* lead to filamentous growth: regulation by starvation and RAS. *Cell* **68**:1077-1090.
- Guthrie, C., and G. R. Fink (ed.). 1991. *Methods in enzymology*, vol. 194. Academic Press, Inc., San Diego, Calif.
- Hasson, M. S., D. Blinder, J. Thorner, and D. D. Jenness. 1994. Mutational activation of the STE5 gene product bypasses the requirement for G protein beta and gamma subunits in the yeast pheromone response pathway. *Mol. Cell Biol.* **14**:1054-1065.
- Healy, A. M., S. Zolnierowicz, A. E. Stapleton, M. Goebel, A. A. DePaoli-Roach, and J. R. Pringle. 1991. *CDC55*, a *Saccharomyces cerevisiae* gene involved in cellular morphogenesis: identification, characterization, and homology to the B subunit of mammalian type 2A protein phosphatases. *Mol. Cell Biol.* **11**:5767-5780.
- Herskowitz, I. 1995. MAP kinase pathways in yeast: for mating and more. *Cell* **80**:187-197.
- Higgins, J. B., and P. J. Casey. 1994. *In vitro* processing of recombinant G protein γ subunits. Requirements for assembly of an active $\beta\gamma$ complex. *J. Biol. Chem.* **269**:9067-9073.
- Hoffman, C. S., and F. Winston. 1987. A ten-minute DNA preparation from yeast efficiently releases autonomous plasmids for transformation of *Escherichia coli*. *Gene* **57**:267-272.
- Hollenberg, S. M., R. Sternglanz, P. F. Cheng, and H. Weintraub. 1995. Identification of a new family of tissue-specific basic helix-loop-helix proteins with a two-hybrid system. *Mol. Cell Biol.* **15**:3813-3822.
- Jackson, C. L., and L. H. Hartwell. 1990. Courtship in *S. cerevisiae*: both cell types choose mating partners by responding to the strongest pheromone signal. *Cell* **63**:1039-1051.
- Jackson, C. L., and L. H. Hartwell. 1990. Courtship in *Saccharomyces cerevisiae*: an early cell-cell interaction during mating. *Mol. Cell Biol.* **10**:2202-2213.
- Jackson, C. L., J. B. Konopka, and L. H. Hartwell. 1991. *S. cerevisiae* α pheromone receptors activate a novel signal transduction pathway for mating partner discrimination. *Cell* **67**:389-402.
- Johnson, D. L., and J. R. Pringle. 1990. Molecular characterization of a *CDC42*, a *Saccharomyces cerevisiae* gene involved in the development of cell polarity. *J. Cell Biol.* **111**:143-152.
- Kang, Y. S., J. Kane, J. Kurjan, J. M. Stadel, and D. J. Tipper. 1990. Effects of expression of mammalian G α and hybrid mammalian-yeast G α proteins on the yeast pheromone response signal transduction pathway. *Mol. Cell Biol.* **10**:2582-2590.
- Kao, L.-R., J. Peterson, R. Ji, L. Bender, and A. Bender. 1996. Interactions between the ankyrin repeat-containing protein Akrlp and the pheromone response pathway in *Saccharomyces cerevisiae*. *Mol. Cell Biol.* **16**:168-178.
- Kranz, J. E., B. Satterberg, and E. A. Elion. 1994. The MAP kinase Fus3 associates with and phosphorylates the upstream signaling component Ste5. *Genes Dev.* **8**:313-327.
- Kron, S. J., C. A. Styles, and G. R. Fink. 1994. Symmetric cell division in pseudohyphae of the yeast *Saccharomyces cerevisiae*. *Mol. Biol. Cell* **5**:1003-1022.
- Kurjan, J. 1985. α -Factor structural gene mutations in *Saccharomyces cerevisiae*: effects on α -factor production and mating. *Mol. Cell Biol.* **5**:787-796.
- Kurjan, J. 1993. The pheromone response pathway in *Saccharomyces cerevisiae*. *Annu. Rev. Genet.* **27**:147-179.
- Leberer, E., D. Dignard, D. Harcus, D. Y. Thomas, and M. Whiteway. 1992. The protein kinase homologue Ste20p is required to link the yeast pheromone response G-protein $\beta\gamma$ subunits to downstream signalling components. *EMBO J.* **11**:4815-4824.
- Leberer, E., D. Dignard, L. Hougau, D. Y. Thomas, and M. Whiteway. 1992. Dominant-negative mutants of a yeast G-protein β subunit identify two functional regions involved in pheromone signalling. *EMBO J.* **11**:4805-4813.
- Legrain, P., M.-C. Dokhelar, and C. Transy. 1994. Detection of protein-protein interactions using different vectors in the two-hybrid system. *Nucleic Acids Res.* **22**:3241-3242.
- Liu, H., C. A. Styles, and G. R. Fink. 1993. Elements of the yeast pheromone response pathway required for filamentous growth of diploids. *Science* **262**:1741-1744.

51. Marcus, S., A. Polverino, M. Bar, and M. Wigler. 1994. Complexes between STE5 and components of the pheromone-responsive mitogen-activated protein kinase module. *Proc. Natl. Acad. Sci. USA* **91**:7762–7766.
52. Michaelis, S., and I. Herskowitz. 1988. The α -factor pheromone of *Saccharomyces cerevisiae* is essential for mating. *Mol. Cell. Biol.* **8**:1309–1318.
53. Michaely, P., and V. Bennett. 1992. The ANK repeat: a ubiquitous motif involved in macromolecular recognition. *Trends Cell Biol.* **2**:127–129.
54. Miller, J. H. 1972. Experiments in molecular genetics. Cold Spring Harbor Laboratory, Cold Spring Harbor, N.Y.
55. Miyajima, I., K. Arai, and K. Matsumoto. 1989. *GPA1*^{Val-50} mutation in the mating-factor signaling pathway in *Saccharomyces cerevisiae*. *Mol. Cell. Biol.* **9**:2289–2297.
56. Neiman, A. M., and I. Herskowitz. 1994. Reconstitution of a yeast protein kinase cascade *in vitro*: activation of the yeast MEK homologue STE7 by STE11. *Proc. Natl. Acad. Sci. USA* **91**:3398–3402.
57. Peter, M., A. Gartner, J. Horecka, G. Ammerer, and I. Herskowitz. 1993. FAR1 links the signal transduction pathway to the cell cycle machinery in yeast. *Cell* **73**:747–760.
58. Printen, J. A., and G. F. Sprague, Jr. 1994. Protein-protein interactions in the yeast pheromone response pathway: Ste5p interacts with all members of the MAP kinase cascade. *Genetics* **138**:609–619.
59. Pryciak, P. M., and L. H. Hartwell. Unpublished observations.
60. Pryciak, P. M., K. Schrick, and L. H. Hartwell. Unpublished observations.
61. Pryciak, P. M., B. R. Thornton, and L. H. Hartwell. Unpublished observations.
62. Ramer, S. W., and R. W. Davis. 1993. A dominant truncation allele identifies a gene, *STE20*, that encodes a putative protein kinase necessary for mating in *Saccharomyces cerevisiae*. *Proc. Natl. Acad. Sci. USA* **90**:452–456.
63. Ramer, S. W., S. J. Elledge, and R. W. Davis. 1992. Dominant genetics using a yeast genomic library under the control of a strong inducible promoter. *Proc. Natl. Acad. Sci. USA* **89**:11589–11593.
64. Reid, B. J., and L. H. Hartwell. 1977. Regulation of mating in the cell cycle of *Saccharomyces cerevisiae*. *J. Cell Biol.* **75**:355–365.
65. Roberts, R. L., and G. R. Fink. 1994. Elements of a single MAP kinase cascade in *Saccharomyces cerevisiae* mediate two developmental programs in the same cell type: mating and invasive growth. *Genes Dev.* **8**:2974–2985.
66. Ronne, H., M. Carlberg, G.-Z. Hu, and J. O. Nehlin. 1991. Protein phosphatase 2A in *Saccharomyces cerevisiae*: effects on cell growth and bud morphogenesis. *Mol. Cell. Biol.* **11**:4876–4884.
67. Schrick, K. 1994. Ph.D. thesis. University of Washington, Seattle.
68. Segall, J. E. 1993. Polarization of yeast cells in spatial gradients of alpha mating factor. *Proc. Natl. Acad. Sci. USA* **90**:8332–8336.
69. Sherman, F. 1991. Getting started with yeast. *Methods Enzymol.* **194**:3–21.
70. Sikorski, R. S., and P. Hieter. 1989. A system of shuttle vectors and yeast host strains designed for efficient manipulation of DNA in *Saccharomyces cerevisiae*. *Genetics* **122**:19–27.
71. Simon, M.-N., C. DeVirgilio, B. Souza, J. R. Pringle, A. Abo, and S. I. Reed. 1995. Role for the Rho-family GTPase Cdc42 in yeast mating-pheromone signal pathway. *Nature (London)* **376**:702–705.
72. Simonds, W. F., J. E. Butrynski, N. Gautam, C. G. Unson, and A. M. Spiegel. 1991. G-protein $\beta\gamma$ dimers. Membrane targeting requires subunit coexpression and intact gamma C-A-A-X domain. *J. Biol. Chem.* **266**:5363–5366.
73. Sloat, B. F., A. Adams, and J. R. Pringle. 1981. Roles of the *CDC24* gene product in cellular morphogenesis during the *Saccharomyces cerevisiae* cell cycle. *J. Cell Biol.* **89**:395–405.
74. Spain, B. H., D. Koo, M. Ramakrishnan, B. Dzudzor, and J. Colicelli. 1995. Truncated forms of a novel yeast protein suppress the lethality of a G protein α subunit deficiency by interacting with the β subunit. *J. Biol. Chem.* **270**:25435–25444.
75. Sprague, G. F., Jr. 1991. Assay of yeast mating reaction. *Methods Enzymol.* **194**:77–93.
76. Sprague, G. F., Jr., and J. W. Thorner. 1992. Pheromone response and signal transduction during the mating process of *Saccharomyces cerevisiae*, p. 657–744. In E. W. Jones, J. R. Pringle, and J. R. Broach (ed.), *The molecular and cellular biology of the yeast Saccharomyces*, vol. 2. Cold Spring Harbor Laboratory Press, Cold Spring Harbor, N.Y.
77. Stevenson, B. J., B. Ferguson, C. DeVirgilio, E. Bi, J. R. Pringle, G. Ammerer, and G. F. Sprague, Jr. 1995. Mutation of *RGAI*, which encodes a putative GTPase-activating protein for the polarity-establishment protein Cdc42p, activates the pheromone response pathway in the yeast *Saccharomyces cerevisiae*. *Genes Dev.* **9**:2949–2963.
78. Stevenson, B. J., N. Rhodes, B. Errede, and G. F. Sprague, Jr. 1992. Constitutive mutants of the protein kinase STE11 activate the yeast pheromone response pathway in the absence of the G protein. *Genes Dev.* **6**:1293–1304.
79. Stone, D. E., and S. I. Reed. 1990. G protein mutations that alter the pheromone response in *Saccharomyces cerevisiae*. *Mol. Cell. Biol.* **10**:4439–4446.
80. Stotz, A., and P. Linder. 1990. The *ADE2* gene from *Saccharomyces cerevisiae*: sequence and new vectors. *Gene* **95**:91–98.
81. Touhara, K., B. E. Hawes, T. vanBiesen, and R. J. Lefkowitz. 1995. G protein $\beta\gamma$ subunits stimulate phosphorylation of Shc adapter protein. *Proc. Natl. Acad. Sci. USA* **92**:9284–9287.
82. Trueheart, J., J. D. Boeke, and G. R. Fink. 1987. Two genes required for cell fusion during yeast conjugation: evidence for a pheromone-induced surface protein. *Mol. Cell. Biol.* **7**:2316–2328.
83. vanBiesen, T., B. E. Hawes, D. K. Luttrell, K. M. Krueger, K. Touhara, E. Porfiri, M. Sakaue, L. M. Luttrell, and R. J. Lefkowitz. 1995. Receptor-tyrosine-kinase- and G $\beta\gamma$ -mediated MAP kinase activation by a common signalling pathway. *Nature (London)* **376**:781–784.
84. van Zyl, W., W. Huang, A. A. Sneddon, M. Stark, S. Camier, M. Werner, C. Marck, A. Sentenac, and J. R. Broach. 1992. Inactivation of the protein phosphatase 2A regulatory subunit A results in morphological and transcriptional defects in *Saccharomyces cerevisiae*. *Mol. Cell. Biol.* **12**:4946–4959.
85. Whiteway, M., K. L. Clark, E. Leberer, D. Dignard, and D. Y. Thomas. 1994. Genetic identification of residues involved in association of α and β G-protein subunits. *Mol. Cell. Biol.* **14**:3223–3229.
86. Whiteway, M., L. Hougan, D. Dignard, D. Y. Thomas, L. Bell, G. C. Saari, F. J. Grant, P. O'Hara, and V. L. MacKay. 1989. The *STE4* and *STE18* genes of yeast encode potential β and γ subunits of the mating factor receptor-coupled G protein. *Cell* **56**:467–477.
87. Whiteway, M., L. Hougan, and D. Y. Thomas. 1990. Overexpression of the *STE4* gene leads to mating response in haploid *Saccharomyces cerevisiae*. *Mol. Cell. Biol.* **10**:217–222.
88. Whiteway, M. S., C. Wu, T. Leeuw, K. Clark, A. Fourest-Lieuvain, D. Y. Thomas, and E. Leberer. 1995. Association of the yeast pheromone response G protein $\beta\gamma$ subunits with the MAP kinase scaffold Ste5p. *Science* **269**:1572–1575.
89. Wu, C., M. Whiteway, D. Y. Thomas, and E. Leberer. 1995. Molecular characterization of Ste20p, a potential mitogen-activated protein or extracellular signal-regulated kinase kinase (MEK) kinase kinase from *Saccharomyces cerevisiae*. *J. Biol. Chem.* **270**:15984–15992.
90. Zhao, Z.-S., T. Leung, E. Manser, and L. Lim. 1995. Pheromone signalling in *Saccharomyces cerevisiae* requires the small GTP-binding protein Cdc42p and its activator *CDC24*. *Mol. Cell. Biol.* **15**:5246–5257.
91. Zhou, Z., A. Gartner, R. Cade, G. Ammerer, and B. Errede. 1993. Pheromone-induced signal transduction in *Saccharomyces cerevisiae* requires the sequential function of three protein kinases. *Mol. Cell. Biol.* **13**:2069–2080.
92. Ziman, M., J. M. O'Brien, L. A. Ouellette, W. R. Church, and D. I. Johnson. 1991. Mutational analysis of *CDC42Sc*, a *Saccharomyces cerevisiae* gene that encodes a putative GTP-binding protein involved in the control of cell polarity. *Mol. Cell. Biol.* **11**:3537–3544.